An Adaptive Corridor–Wide Signal Timing Optimization Methodology for Traffic Network with Multiple Highway-Rail Grade Crossings

Yifeng Chen, MS
Graduate Research Assistant
Department of Civil Engineering
University of Nebraska-Lincoln

Laurence R. Rilett, Ph.D.
Keith W. Klaasmeyer Chair in Engineering and Technology
Distinguished Professor
Department of Civil Engineering
University of Nebraska-Lincoln

Technical Report Documentation Page

1. Report No. 26-1121-0018-005	2. Government Accession No.	3. Recipient's Catalog No.
4. Title and Subtitle An Adaptive Corridor–Wide Signal Timing Optimization Methodology for Traffic Network with Multiple Highway-Rail Grade Crossings		5. Report Date June 2016
		6. Performing Organization Code
7. Author(s) Yifeng Chen and Laurence R. Rilett		8. Performing Organization Report No. 26-1121-0018-005
9. Performing Organization Name and Address Nebraska Transportation Center 2200 Vine St. PO Box 830851 Lincoln, NE 68583-0851		10. Work Unit No. (TRAIS)
		11. Contract or Grant No. DTRT13-G-UTC59
12. Sponsoring Agency Name and Address University Transportation Center for Railway Safety (UTCRS) University of Texas Rio Grande Valley (UTRGV) 1201 W. University Dr. Edinburg, TX 78539		13. Type of Report and Period Covered Final Report November 2013 – June 2016
		14. Sponsoring Agency Code USDOT UTC Program
15. Supplementary Notes		

16. Abstract
Highway-rail grade crossings (HRGCs) and the intersections in their proximity are areas where potential problems in terms of safety and efficiency often arise if only simple or outdated treatments, such as normal signal timing or passive railroad warning signs, are utilized. When it comes to a corridor or a network with multiple HRGCs and heavy train traffic, the problems will be more complicated due to randomness of train arrivals and frequent abruptions of normal signal timing operation of the whole corridor. This report develops a methodology of signal timing optimization that is specially designed for such a corridor/network. Due to high time and money costs associated with testing the methodology in the field, and safety issues related to field experiments, the proposed optimization program was instead developed, used, and evaluated in a micro-simulation environment using the VISSIM simulation software package. To replicate field conditions, real train data has been collected from the field test bed using advanced train detection technologies and input into the simulation models. Moreover, the stochastic nature of traffic has been considered in the simulation experiment by conducting multiple simulation runs with random seeds. Based on the research results, it can be concluded that the methodology can significantly improve both the safety and efficiency of the study corridor with HRGCs in both offline and online scenarios, however, at the cost of higher network delay. The effects of the prediction errors on the safety and operation of the study network are also analyzed.

17. Key Words Highway-railway grade crossing, HRGC, traffic preemption strategies, corridor traffic signal optimization		18. Distribution Statement		
19. Security Classif. (of this report) Unclassified	20. Security Classif. (of this page) Unclassified		21. No. of Pages 63	22. Price

Table of Contents

List of Figures

List of Tables

Acknowledgements

Abstract

Highway-rail grade crossings (HRGCs) and the intersections in their proximity are areas where potential problems in terms of safety and efficiency often arise if only simple or outdated treatments, such as normal signal timing or passive railroad warning signs, are utilized. When it comes to a corridor or a network with multiple HRGCs and heavy train traffic, the problems will be more complicated due to randomness of train arrivals and frequent abruptions of normal signal timing operation of the whole corridor. This report develops a methodology of signal timing optimization that is specially designed for such a corridor/network. Due to high time and money costs associated with testing the methodology in the field, and safety issues related to field experiments, the proposed optimization program was instead developed, used, and evaluated in a micro-simulation environment using the VISSIM simulation software package. To replicate field conditions, real train data has been collected from the field test bed using advanced train detection technologies and input into the simulation models. Moreover, the stochastic nature of traffic has been considered in the simulation experiment by conducting multiple simulation runs with random seeds. Based on the research results, it can be concluded that the methodology can significantly improve both the safety and efficiency of the study corridor with HRGCs in both offline and online scenarios, however, at the cost of higher network delay. The effects of the prediction errors on the safety and operation of the study network are also analyzed.

Chapter 1 Introduction

Signal control has profound impact on traffic flow characteristics and the roadway network performance. A good coordinated signal control system can enhance roadway safety and efficiency. However, problems can arise in the case of a multimodal network with sudden random transitions among different modes of traffic (e.g. a system with railroads intersecting roadways at grade). When a train is passing a highway-rail grade crossing (HRGC), the signals at intersections near the crossing transfer from their normal operation mode to the preemption mode, which prohibits movements over the tracks and allows other movements to occur (1). Long queues could accumulate at the intersections in the vicinity of a grade crossing after the passing of a long train, and the queues might propagate to upstream intersections as well.

Frequent preemptions at highway-rail grade crossings can significantly interrupt coordinated traffic flows and thus seriously degrade the efficiency of adjacent signal controlled intersections, especially when they are operating at or close to capacity (2). Moreover, the inability of traffic control to warn train drivers of hazardous crossing conditions can result in fatality-causing accidents at grade crossings (2). As a result, the safety and efficiency of the whole network might be degraded significantly.

It should be noted that standard traffic signal optimization approaches do not apply for solving these problems because most signal strategies at intersections near HRGCs differ from those at normal signalized intersections that do not experience the interruption of trains (2). There are a number of studies that modeled the interaction of traffic signals at intersections close to HRGCs with railroad active warning devices (3-9). Most of the work has focused on traffic signal preemption strategies, their related train detection techniques, and train arrival prediction methods. Although much research has been completed regarding signal optimization for single

1

intersections, traffic corridors, and traffic networks, few of them have considered the impact of preemption strategies. To improve the performance and safety of corridor-wide traffic control, the integration of current or future preemption strategies in a corridor-wide signal control setting is needed. The motivation of this research is to bridge the gap between corridor-wide signal optimization and railroad preemption strategies, or in other words, to integrate railroad preemption strategies with corridor-wide signal optimization.

Further, current signal control themes and rail preemption strategies do not always consider the dynamics of traffic demand and route choice behavior of travelers. If traffic conditions such as signal timing, delay at intersections, or train arrivals are changing, the routes of travelers will also change in a short time interval. Therefore, one of the objectives of this research is to develop an adaptive traffic signal optimization methodology that can promptly respond to the dynamic routing of travelers.

1.1 Background

1.1.1 Highway-Rail Grade Crossing and the Nearby Intersections

Highway-Rail Grade Crossings (HRGCs) are locations where roadway and rail intersect. This report is concerned with highway-rail grade crossings near a signalized intersection, as shown in Figure 1.1. The area bounded by the dotted line includes a crossing roadway, a parallel roadway, the rail track, and active warning devices, including flashing lights and automatic gates.
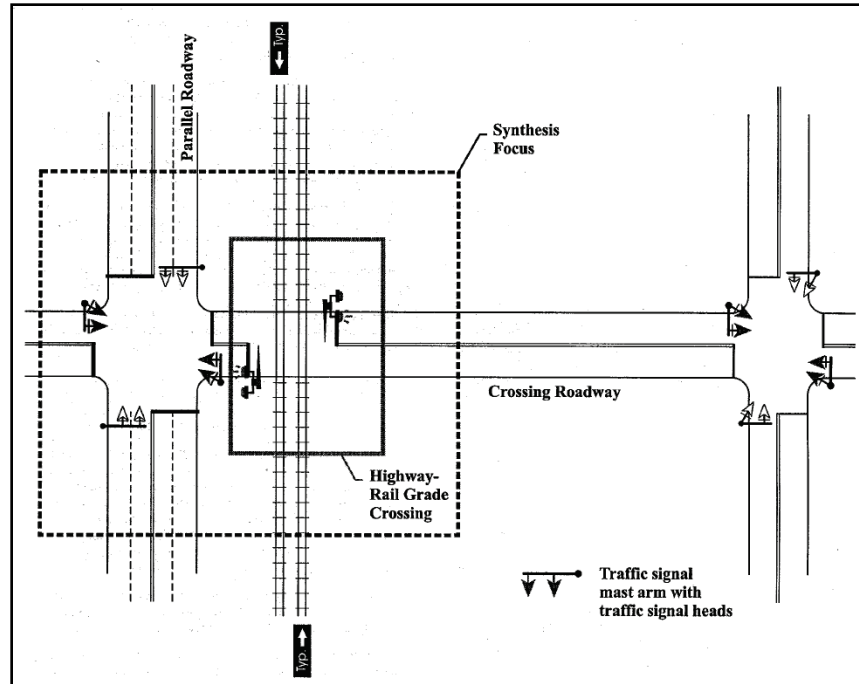
Figure 1.1 Highway-rail grade crossing near a signalized intersection (11)

1.1.2 Signal Control at and near Highway-Rail Grade Crossings

At HRGCs, both active and passive warning devices are implemented to warn drivers of train arrivals. For signalized intersections, preemption is used to clear traffic crossing the railway track before the arrival of a train. A key point for the safety and efficiency of the HRGC is the communication and cooperation between the active warning devices from the railroad and the signal preemption from the highway system. The current standard preemption (SP) strategy (12) and the constant warning time (CWT) detection system cannot estimate the fluctuation of train speeds perfectly, which results in excessive vehicle delay and safety problems with pedestrians at intersections near HRGCs (12).

1.2 Research Objective

The first objective of this research is to improve the safety at intersections near the HRGCs (IHRGCs) on the studied corridor. The chances of crossing pedestrian phase cutoffs

upon preemption should be reduced or eliminated. The secondary objective of this research is to improve the efficiency of traffic operation at and near HRGCs on this corridor. The vehicular congestion and delay in the corridor are expected to be reduced, therefore improving safety. To achieve these goals, the research focuses on:

1) developing a simulation model of the studied corridor/network, which will be calibrated using field data;

2) developing and coding an algorithm for optimizing corridor signal timings;

3) collecting train data from the field and developing a train arrival prediction model;

4) developing a new transition preemption strategy (TPS) algorithm for multiple railroad tracks and multiple HRGCs with multiple crossing trains, then incorporating the algorithm into corridor signal timing optimization; and

5) designing a simulation experiment and conducting a sensitivity analysis to evaluate the effectiveness of the proposed methodology with different simulation scenarios. The case study will be done using a test bed in Lincoln, Nebraska.

Chapter 2 Literature Review

2.1 Traffic Control Systems at or near Highway-Rail Grade Crossings

2.1.1 Traffic Control Devices at HRGCs

There are two categories of traffic control devices at HRGCs: passive control devices and active control devices (10). Advance warning signs, pavement markings, and crossbucks are passive control devices that identify and warn road users of the existence of a grade crossing and advise road users to slow down or stop at the grade crossing in order to yield to any rail traffic (1). However, passive warning devices give no indication of the imminent presence of a train.

Active control devices "inform road users of the approach or presence of rail traffic at grade crossings" (1). These devices include flashing lights, bells, and automatic gates. In addition, four quadrant gate systems, traffic control signals, and actuated blank-out and variable message signs are categorized as active control devices (1). Active control devices are activated through train detection technologies as a train is approaching the crossings. When compared to passive control devices, active control devices are proved to effectively reduce accidents and improve safety at HRGCs (6).

2.1.2 Train Detection Technologies

Active control devices are activated through train detection systems. The train detection technologies have developed through three generations. The first generation of train detection systems is based on track circuits, and can detect train presence, direction, and even speed. They are fail-safe, and are the most commonly used in the United States (10, 13). The second generation detection systems can not only detect the presence of a train, but are also able to measure the instantaneous speeds of approaching trains. Generally, second-generation train detection systems are installed off the railroad right-of-way, and are often mounted on poles near the railroad. Radar and video detectors belong to this category. In this research, two second

generation detection systems, a Doppler radar detector, and a video image detector were used to measure train speeds. The third generation systems further provide continuously updated train information as trains are approaching the grade crossing. These systems require on-board global positioning systems (GPS) or other Automated Vehicle Identification (AVI) technology (8). The Positive Train Control (PTC) system is a typical example of this generation.

2.2 Preemption of Signal Controller at HRGCs

2.2.1 Definition of Preemption

Preemption is defined as the transfer from normal signal operation to a special control mode, which is used when vehicles that may be in danger of being hit by the train need to be cleared from the tracks before the train arrives at the HRGC (6). Other sources that can generate preemption inputs include: drawbridges, emergency vehicles, and transit vehicles. Federal law regulates that, "A highway-rail grade crossing warning system shall be maintained to activate in accordance with the design of the warning system, but in no event shall it provide less than 20 seconds warning time for the normal operation of through trains before the grade crossing is occupied by rail traffic" (16). Therefore, the 20 s minimum preemption is the common practice in the United States, and is referred to as the Minimum Warning Time (MWT), which is a minimum time requirement by the above guidelines. In reality, the actual railroad warning time is usually longer than the MWT for safety reasons, especially in case of wide multi-track crossings, or when a longer MWT is required by the highway authority (17).

2.2.2 When to Use Preemption

While it is illegal for vehicles to stop on the tracks even when no train is coming, many drivers choose to do so either due to their impatience, or because they were caught in a queue spilling back from the approach during a red signal phase at the intersection ahead (17). There are two general conditions in which preemption should be considered (14):

6

A. highway traffic queues have the potential for extending across a rail crossing nearby, and

B. traffic spilling up from a nearby downstream railroad crossing could interfere with signalized intersections.

The Manual on Uniform Traffic Control Devices (MUTCD) requires that when the HRGCs are within 200 feet (65m) of a signalized intersection, preemption should be considered at this site (MUTCD, 2009). However, experience indicates that this distance can often be exceeded, and the need for preemption should be based on a detailed analysis and engineer judgments with respect to queuing analysis, traffic volumes, number of lanes, traffic signal timing, saturation flow rates, vehicle classes, etc., rather than a predetermined distance such as 200 feet (65 m) (10, 14).

2.2.3 Preemption Sequence

Generally, current signal controllers have a five-step preemption sequence (8, 18): entry into preemption, termination of the current phase, start of track clearance phase, preemption hold interval, and return to normal operation. It should be noted that controllers from different manufacturers may have differences in configurations and operations for the above five steps, which are defined as preemption capabilities in Marshall and Berg (19).

2.2.4 Preemption Design of Signal Controllers at HRGCs

There are two types of preemption designs: simultaneous preemption and advance preemption (14, 15, 17). Under simultaneous preemption the signal controller is notified of the approaching train and starts the preemption sequence at the same time that the railway warning devices are activated; under advance preemption, the signal controller receives the preemption call before the active warning devices are activated (14, 15, 17). The time difference between the start of the preemption sequence at the signal controller and the activation of the active warning

devices is called the advance preemption time (17). Note that for simultaneous preemption the advance preemption time is zero.

2.2.5 Preemption Trap

For an advance preemption strategy, it is possible for the track clearance phase to end before the gate is down. In this case, drivers are unaware of the end of the track clearance phase and the incoming train because there are no warning lights or descending gates. Consequently, vehicles will continue to cross the tracks and stop at the intersection. When the crossing gates are down, vehicles may be trapped between the stop line of the intersection and the rail tracks, or even stopped on the tracks if the queue is long enough. This is called a "preemption trap," which exposes drivers to unsafe conditions (17, 20). Some potential solutions for a preempt trap include increasing the track clearance green time, using two preempts with "gate down" confirmation, and controlling variation in advance preemption time and the right-of-way transfer time (8, 17, 20).

Chapter 3 Methodology

3.1 Proposed Methodology

The proposed optimization methodology is an integrated simulation-based approach. The architecture of the methodology consists of two modules: a simulation module and an optimization module. The simulation module is a VISSIM-based simulation model. The VISSIM simulator can replicate the traffic in the field, including vehicles, pedestrians, and trains. The performance evaluator in VISSIM outputs traffic system performance metrics including average delay, number of stops, and queue length, as well as train information including train speed, train length, and train travel time. The optimization module consists of a GA-based optimizer, a train arrival time prediction model, and a preemption logic algorithm. The train arrival time prediction model is used to predict train arrival times at downstream HRGCs at set intervals. The default update time is one second. The predicted arrival time is sent to the preemption algorithm. A new preemption logic algorithm is proposed in this report and is loaded in this module. The optimizer identifies the best signal timings based on the constraints of the signal controller logic and preemption logic. An interface is created that connects the two modules and manages the interchange of data between them. During the optimization, the simulation module sends the system performance measures and train information to the optimization module, while the optimization module generates candidate signal timing plans and sends them to the simulation module for evaluation. The best solution is identified among these signal timing candidates.

3.2 Test Network

The test study network for this research is a 2.4 km by 3.2 km urban road network in Lincoln, Nebraska, as shown in Figure 3.1. The network is bounded on the west by North 27th Street, on the east by North 48th Street, on the north by Superior Street, and on the south by Holdrege Street. A 3.2 km long Burlington Northern Santa Fe (BNSF) railroad is located from

the northeast corner to the southwest corner of the test network. This is a dual-track mainline railroad. There is an overpass on North 27th Street, and an underpass on North 48th Street, as shown in Figure 3.1. These points form the western and eastern geographic boundaries of the network, respectively. Superior Street and Holdrege Street form the northern and southern boundaries of the network, respectively.

Between the overpass at 27th Street and the underpass at 48th Street, there are three at-grade railroad crossings on North 33rd Street, Adams Street, and North 44 Street respectively. They are marked as "H1," "H2," and "H3" in Figure 3.1. There are three intersections near the three HRGCs: 33rd Street and Cornhusker Highway, 35th Street and Cornhusker Highway, and 44th Street and Cornhusker Highway. They are referred to as study/target intersections in Figure 3.1 and throughout the report.

In Figure 3.1, the test corridor is indicated by the blue oval, which includes Cornhusker Highway (Highway 6), the BNSF railroad line, and the three HRGCs along Cornhusker Highway. Cornhusker Highway runs parallel to the BNSF railroad after the Adams Street HRGC. There are a total of six intersections along the test corridor: 27th Street and Cornhusker Highway, 29th Street and Cornhusker Highway, 33rd Street and Cornhusker Highway, 35th Street and Cornhusker Highway, 44th Street and Cornhusker Highway, and 48th Street and Cornhusker Highway. Three of them are in the proximity of a HRGC, and are regarded as study/target intersections as discussed above.

This corridor was chosen as the test bed because: 1) Cornhusker Highway is a major arterial in Lincoln, and an alternative route to I-80 between Lincoln and Omaha, Nebraska, and the traffic, especially truck traffic, is high on this route; 2) there are approximately 50 to 70 trains per day traveling on the BNSF railroad line, and this volume is increasing (11); 3) the Adams

Street HRGC has been rated as one of the most hazardous HRGCs in Lincoln by the FRA's Web

Accident Prediction System (WBAPS) (21); 4) this corridor is the UNL HRGC test bed system

and is heavily instrumented; and 5) this corridor is close to the University of Nebraska, Lincoln.

In summary, safety and efficiency are critical problems for this corridor, because of high

roadway and railway traffic.
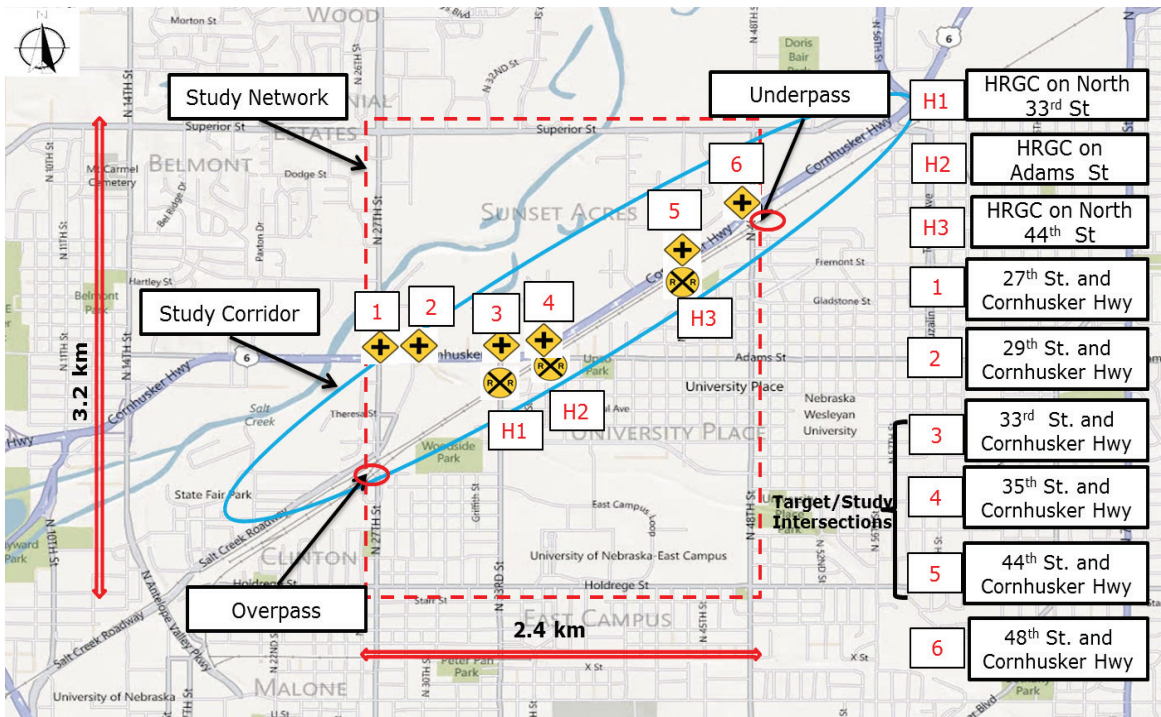
Figure 3.1 Map of the study network

Chapter 4 Train Data Collection and Processing

The purpose of the data collection is to obtain train data that is needed for: 1) the simulation model parameter calibration, and 2) the train arrival prediction model in the optimization module of the proposed methodology. Average train speed, train length, and train frequency are required for the simulation model calibration. In addition, upstream train speed profiles, train acceleration/deceleration rates, and train lengths are required for train arrival prediction. Arrival times of trains at the HRGCs are necessary for the calibration and validation of the prediction models.

4.1 Data Collection Sites

To obtain train information, two upstream locations and one HRGC location in the NTC railroad test bed were chosen as data collection sites. Figure 4.1 shows the two upstream locations (location A and location B) and the Adams Street HRGC (H2). Location A at Salt Creek was set up to collect EB train data, while location B near Superior Street collected WB train data. The Adams Street HRGC was selected for collecting train arrival information. Second generation train detection technologies (e.g. radar and Autoscope video detection) were installed at locations A and B for data collection.
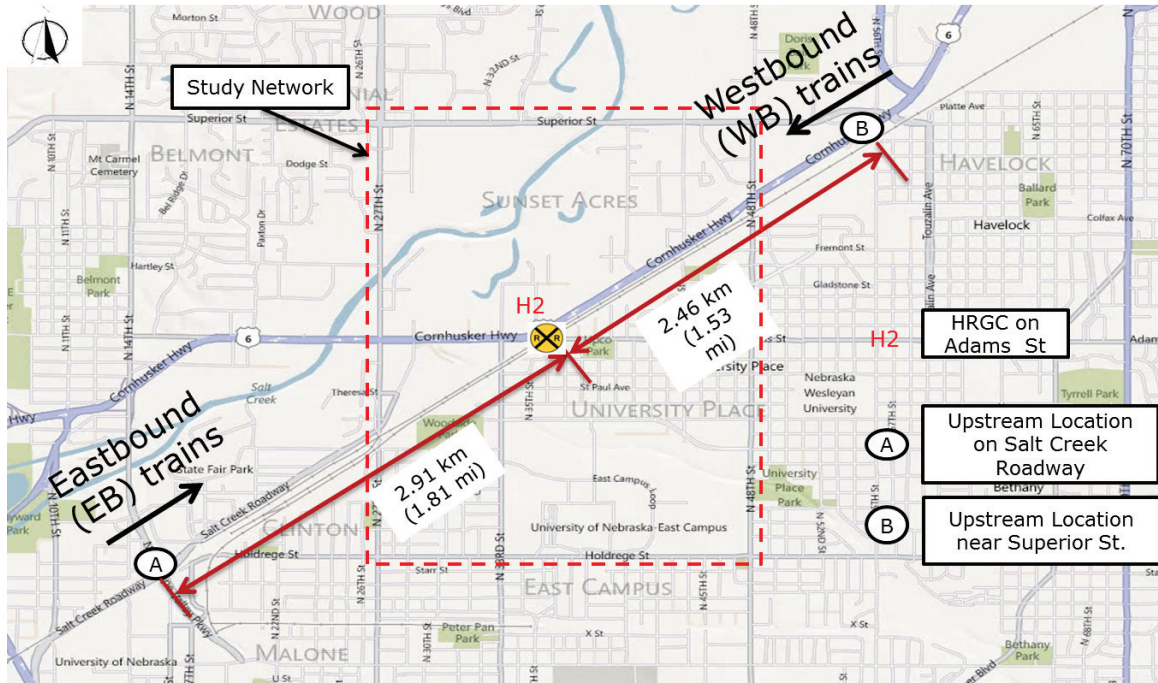
Figure 4.1 Map of the data collection sites

4.2 Data Collection and Processing Methodology

The speed data collection and processing method consists of three parts: 1) online data collection, 2) offline data processing, and 3) offline detector calibration.

4.3 Calibration of Video and Radar Detectors

Both the Autoscope and Doppler radar systems require the use of a multiplicative factor for speed calibration. A linear regression method was used to obtain the calibration factors.

4.3.1 Results of Detector Calibration

Table 4.1 lists the calibration factors of radar and Autoscope video detectors for EB trains. The R-square values of all regression models are close to one, indicating a good fit of the regression line to the ground-truth data. In addition, the p-value in Table 4.1 shows that there were no statistically significant differences between the manual speeds and the speed

measurements in the validation data sets of the Autoscope and radar detectors at the 95 percent confidence interval (CI).

Table 4.1 Calibration factor k for EB train

Detector	Track	Direction	Calibration Factor	R-square	p-value (95% CI)
Radar	Both	Eastbound	1.318	0.994	0.62
Autoscope	Middle	Eastbound	0.818	0.984	0.58
Autoscope	Outside	Eastbound	0.823	0.988	0.86

Chapter 5 Development of Train Arrival Prediction Models

During the data collection process, which lasted from May 2013 to September 2013, a total of 142 EB trains were sampled. The detectors were calibrated as discussed in section 4.3. Subsequently, the speed profiles were measured at the Salt Creek detection site (i.e. location A in Figure 4.1) and their arrival times were recorded at the Adams Street HRGC (i.e. location C in Figure 4.1). The calibrated speed data and the arrival times were used for developing train arrival prediction models.

5.1 Preliminary Analysis of Train Data

A preliminary study of train characteristics in the test corridor was conducted, including train speed, train arrival time, train passing time, train length, and train detection time. The relationship among the different variables of these characteristics was also analyzed in order to inform the prediction model methodology in the next section. Approximately 80 percent of the trains experience a steady increase in speed indicating they are accelerating as they travel eastbound towards the Adams Street HRGC. In general, the trains that had higher initial speeds experienced higher accelerations.

Results from the preliminary train analysis showed that train arrival time correlated to train speed at the Salt Creek location (location A). Although train detection time appears to be related to arrival time, it is actually a function of train speed and train length. Train length does not seem to relate to arrival time, and train speed should be the effective factor. Therefore, train speed and the rate of speed change will be considered as interest variables in the prediction model.

5.2 Prediction Models

A total of 138 trains were used to calibrate and validate the prediction models. These trains do not include those which have stopped before arriving at the Adams St HRGC.

15

Subsequently, 100 trains out of the 138 were randomly selected and used to develop the train arrival prediction models. The remaining 38 trains were used to validate the prediction models.

Two model types were used in the analysis. The first type are kinematic models that are based on simple motion equations and use train measurements taken upstream of the HRGC. By definition these are relatively simple models. The second type are regression models that attempt to identify a statistical relationship between train measurements and the train's arrival time at the HRGC. By definition these are more complicated models and can take a considerable amount of time to calibrate and validate.

It was found that as the accuracy of both the kinematic and MLR models increased, the time in detection increased. The regression models were, on average, approximately 40 percent more accurate than the kinematic models based on the calibration data, and 13.1 percent more accurate based on the validation data.

With respect to the feasibility of the model, developing the regression models is a more complex process. These models need sufficient sample size to perform well and would probably need to be recalibrated at regular intervals. On the other hand, the advantage to the kinematic models is that they are extremely easy to implement in the field. Depending on the emphasis on either accuracy or feasibility, both types of models are options for HRGC applications. To overcome the degradation of the regression models due to small sample size, a combined use of the best kinematic and regression models may be appropriate. Intuitively, the best methodology will be a function of the application, the availability of resources, and the desired accuracy.

Chapter 6 Development of Multiple HRGC, Dual Track Transition Preemption Algorithm

In this chapter, an advanced transition preemption strategy algorithm is developed for a dual-track, multiple HRGC corridor. It is known as the transition preemption strategy for dual track (TPS_DT). This algorithm is coded in the VISSIM VAP program so that it may be analyzed using a micro-simulation model. The algorithm is based on the framework of Transition Preemption Strategy 3 (TPS3) developed by Cho (8). The TPS_DT is developed specifically for the dual-track environment where multiple trains may be traveling in the corridor at any one time. In addition, it is developed for a corridor with multiple HRGCs. The TPS_DT utilizes train arrival information provided by the train prediction model developed in chapter 5, and makes signal phase and pedestrian phase decisions based on the estimated time remaining until the standard preemption algorithm is initiated.

6.1 Development of the TPS_DT Algorithm

Before introducing the logic of the algorithm, some parameters that are used throughout the algorithm need to be explained.

The algorithm first identifies the start time for the TPS_DT procedure. Two parameters are required for identifying the start time: the time remaining until the start of TPS_DT for EB trains ($T^l_{1\_EB}$), and the time remaining until the start of TPS_DT for WB trains ($T^l_{1\_wB}$). These are calculated using Equation 6.1 and Equation 6.2, respectively. It may be seen that $T^l_{1\_EB}$ ($T^l_{1\_wB}$) is the difference between the estimated train arrival time $P^l_{k\_EB}$ ($P^l_{k\_WB}$) and the pre-specified advance preemption warning time τ^l_{EB} (τ^l_{WB}). The TPS_DT algorithm will start when either $T^l_{1\_EB}$ or $T^l_{1\_wB}$ is equal to zero. A value of zero indicates that the estimated arrival time is equal to the pre-specified advance preemption warning time (APWT).

$$T_{1\_EB}^{l} = P_{k\_EB}^{l} - \tau_{EB}^{l} \qquad (0.1)$$

$$T_{1\_wB}^{l} = P_{k\_WB}^{l} - \tau_{WB}^{l} \qquad (0.2)$$

where:

$T_{1\_EB}^{l}$: remaining time to the start of TPS_DT for EB trains at the lth HRGC;

$T_{1\_wB}^{l}$: remaining time to the start of TPS_DT for WB trains at the lth HRGC;

$P_{k\_EB}^{l}$: estimated EB train arrival time to the lth HRGC at the end of k seconds after the train was detected by the advanced detector. This parameter is updated every t seconds as the train approaches the crossing. t=1 in this report;

$P_{k\_WB}^{l}$: estimated WB train arrival time to the lth HRGC at the end of k seconds after the train was detected by advanced detector. This parameter is updated every t seconds as the train approaches the crossing. t=1 in this report;

τ_{EB}^{l}: advanced warning preemption time specified for EB trains at the lth HRGC, $\tau_{EB}^{l} \geq 25s$;

τ_{WB}^{l}: advanced warning preemption time specified for WB trains at the lth HRGC, $\tau_{WB}^{l} \geq 25s$; and

l HRGC in the Cornhusker Hwy corridor. l =1,2, 3, where 1=33rd street HRGC, 2=Adams street HRGC, and 3=44th Street HRGC.

As standard practice in the U.S., the estimated train arrival times in equations 6.1 and 6.2, denoted as $P_{k\_EB}^{l}$ for EB trains and $P_{k\_WB}^{l}$ for WB trains, will be updated every second (8). In the TPS_DT algorithm, the train arrival time can be estimated by using the prediction models developed in chapter 5.

The pre-specified advance preemption warning time (APWT) is referred to as τ_{EB}^l for EB trains and τ_{WB}^l for WB trains in equations 6.1 and 6.2. Note that τ_{EB}^l and τ_{WB}^l should be greater than the constant warning time of 25 seconds.

The other two important parameters in the TPS_DT algorithm are the remaining times until the start of standard preemption (SP) for EB and WB trains, which are denoted as $T_{2\_EB}^l$ and $T_{2\_WB}^l$. These are calculated using equations 6.3 and 6.4, respectively. A zero value of these parameters indicates the start of SP and the termination of the TPS_DT algorithm.

$$T_{2\_EB}^l = P_{k\_EB}^l - c \tag{0.3}$$

$$T_{2\_WB}^l = P_{k\_WB}^l - c \tag{0.4}$$

where:

$T_{2\_EB}^l$:   remaining time to the start of standard preemption (SP) for EB trains at the lth HRGC;

$T_{2\_WB}^l$:   remaining time to the start of standard preemption (SP) for WB trains at the lth HRGC; and

c: time subtracted to ensure 25 s of preemption warning time (s) for the test corridor. Here c=26 s.

Consider a given controller with n phases where phases i, j, and k are the current phase, the next phase, and the phase after the next phase, respectively. The following relationships exist:

$$j = i + 1, if\ i < n;\ j = 1, if\ i = n \tag{0.5}$$

$$k = j + 1, if\ j < n;\ k = 1, if\ j = n \tag{0.6}$$

where:

i, j, k: signal phase, $i, j, k \in phase \{1,2,3, \ldots ,n\}$.

The minimum time needed to service the next phase (e.g. phase j) and the necessary minimum time to service the next two phases (e.g. phases j and k) are calculated as follows:

$$M_j = Y_i + R_i + G_j + Y_j + R_j \tag{0.7}$$

$$M_k = M_j + G_k + Y_k + R_k \tag{0.8}$$

where:

Y_i: amber time of current phase i (s);

R_i: all-red interval of current phase (s);

G_j: minimum green time of phase j (s);

M_j: minimum time to service the next phase (phase j) (s); and

M_k: minimum time to service the phase after the next phase (phase k) (s).

The detector calls in phases $i, j,$ and k are denoted as $Call_i$, $Call_j$ and $Call_k$, respectively. Note that these are dummy variables where a value of 0 indicates that there is no call for the phase, and a value of 1 indicates that there is a call for the phase.

6.2 Implementation of the TPS_DT algorithm in VAP

A flow chart of the VAP logic for the TPS_DT algorithm is shown in Figure 6.1. The algorithm is iterative in nature. In this research, the update interval is set to one second. The logic consists of four modules: 1) the normal operation module, 2) the TPS_DT module, 3) the SP module part 1, and 4) the SP module part 2. The normal operation module is for the normal operation when a train is not present in the corridor. The TPS_DT module was coded according to the algorithm developed in section 6.1. The SP module consists of the submodules part 1 and part 2. The SP module part 1 includes termination of the current phases, start of the track clearance phase, and start of the dwell phases, while the SP module part 2 is set up for the start of the exit phases.
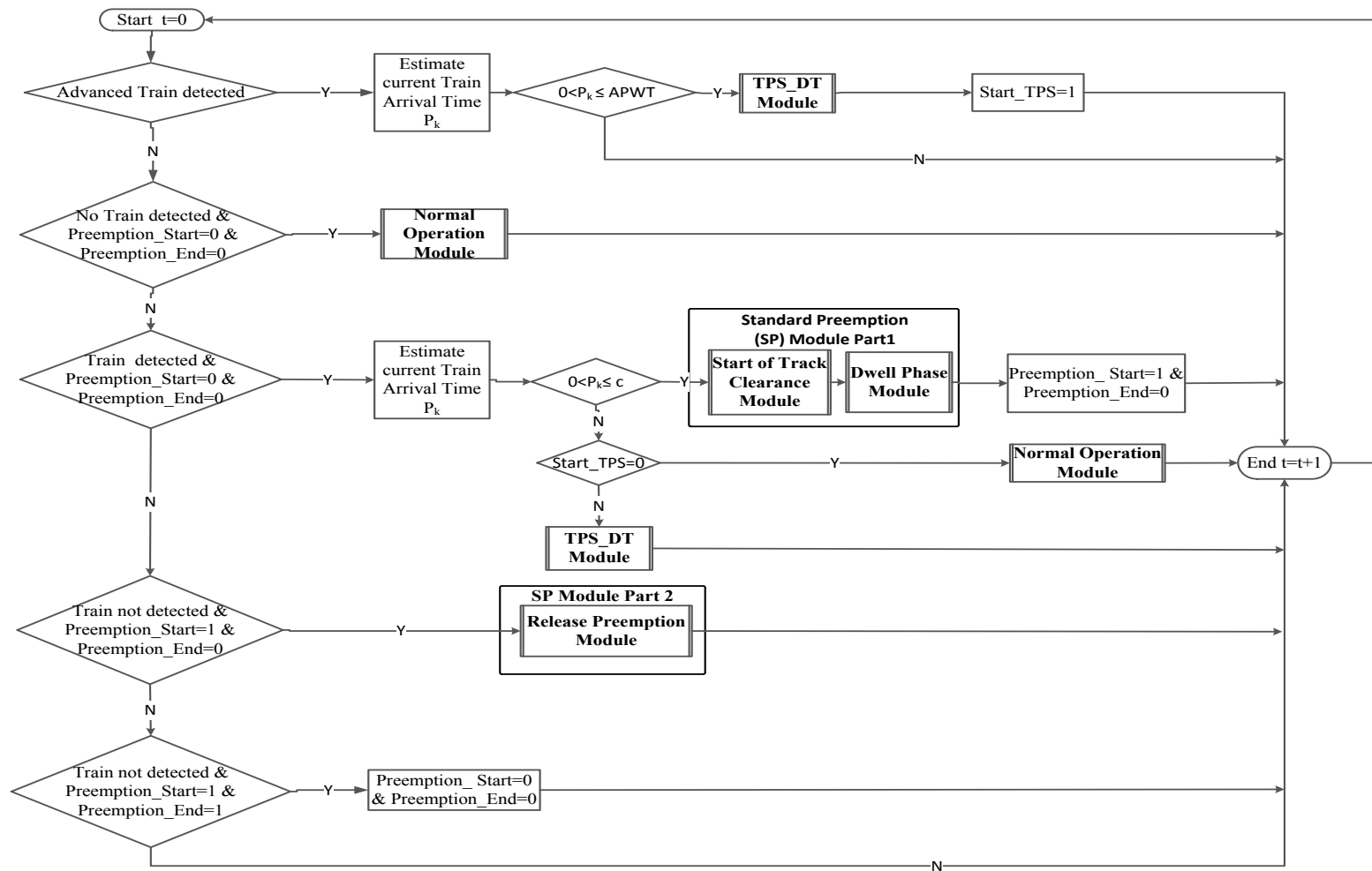
Figure 6.1 Flow chart of the VAP logic for the TPS_DT algorithm

Figure 6.2 shows a schematic of how the four modules of the VAP logic work for the situations of a single train/two simultaneous trains passing through the HRGC. When no trains are present, the normal operation module is run. When one train is present, the normal operation module will be active until the TPS_DT module is initiated. Three conditions, denoted as C1, C2, and C3, need to be fulfilled in order to start the TPS_DT. These conditions are:

C 1: at least one train has been detected at one of the two upstream detector locations (e.g. location A and location B);

C 2: the estimated train arrival time for any train in the corridor is equal to or less than the advance preemption warning time (APWT) ($0 < P_k \leq APWT$); and

C 3: the detection zone is free of any trains (no SP is in process).

Once the train is detected by the CWT detector, and the estimated train arrival time for any train in the corridor is equal to or less than the constant warning time c ($0 < P_k \leq c$), the VAP logic will exit the TPS_DT module and initiate the SP Part 1 module. This module starts the track clearance phase and subsequently the dwell phases. The SP part 1 module operates until the train clears off the CWT detector. Once this is complete, the VAP logic moves forward to the SP part 2 module, which starts the exit phases and releases the standard preemption (SP). Once the SP procedure is finished, the VAP logic goes back to the normal operation module. The conditions for starting the SP part 1 module, and switching from the SP part 1 module to the SP part 2 module, are exactly the same as those in the standard preemption logic described in section 6.2.
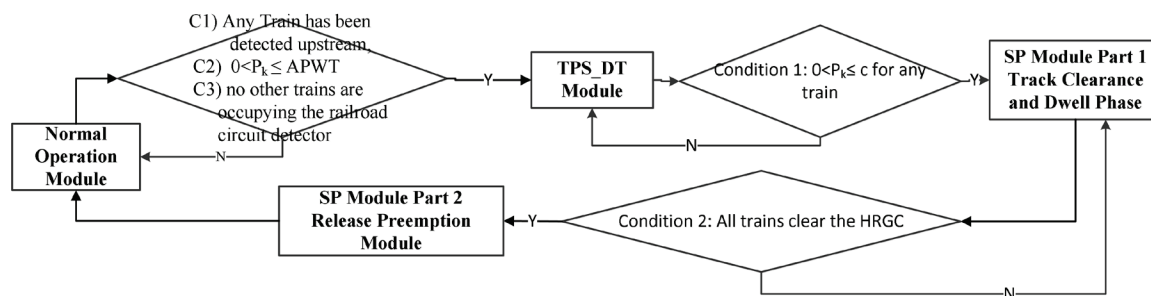
Figure 6.2 Structure of the VAP logic for the TPS_DT algorithm

Figure 6.3 shows a schematic of the train detection system used for the proposed TPS_DT algorithm. It may be seen that there is a detector located at the Salt Creek upstream location for identifying EB trains (location A), and a detector at the location near the 48th Street and Cornhusker Highway for identifying WB trains (location B). The schematic also shows the track circuit system for the CWT preemption at the HRGC. Based on the information obtained at the upstream locations, and the train arrival models developed in chapter 5, the estimated time of arrival can be calculated and used for the algorithm. It may also be seen in Figure 6.3 that all three conditions for starting the TPS_DT module have been met. In particular, train 1 and train 2 have been detected at the upstream locations, and train 2 has reached the position for starting the TPS_DT module. In this case, the TPS_DT module will be initiated by train 2. Note that the position for starting the TPS_DT module is dependent on specific train speed.
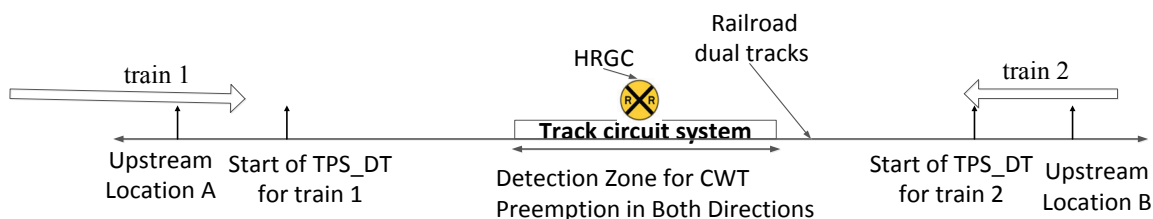
Figure 6.3 Conditions of starting the TPS_DT module

Figure 6.4 shows the time-distance diagram of an example train on this corridor. The x-axis represents time and the y-axis represents distance along the corridor. Without loss of generality, it can be assumed that the train is traveling in the eastbound direction. The train is traveling at a constant speed. Figure 6.4 shows the location of the upstream detector and the location of the railroad detector on the y-axis. The figure also shows the time of the start of the TPS mode and the SP mode on the x-axis. The location and time for the switching between the TPS and SP modes depend on the train's instantaneous speed.
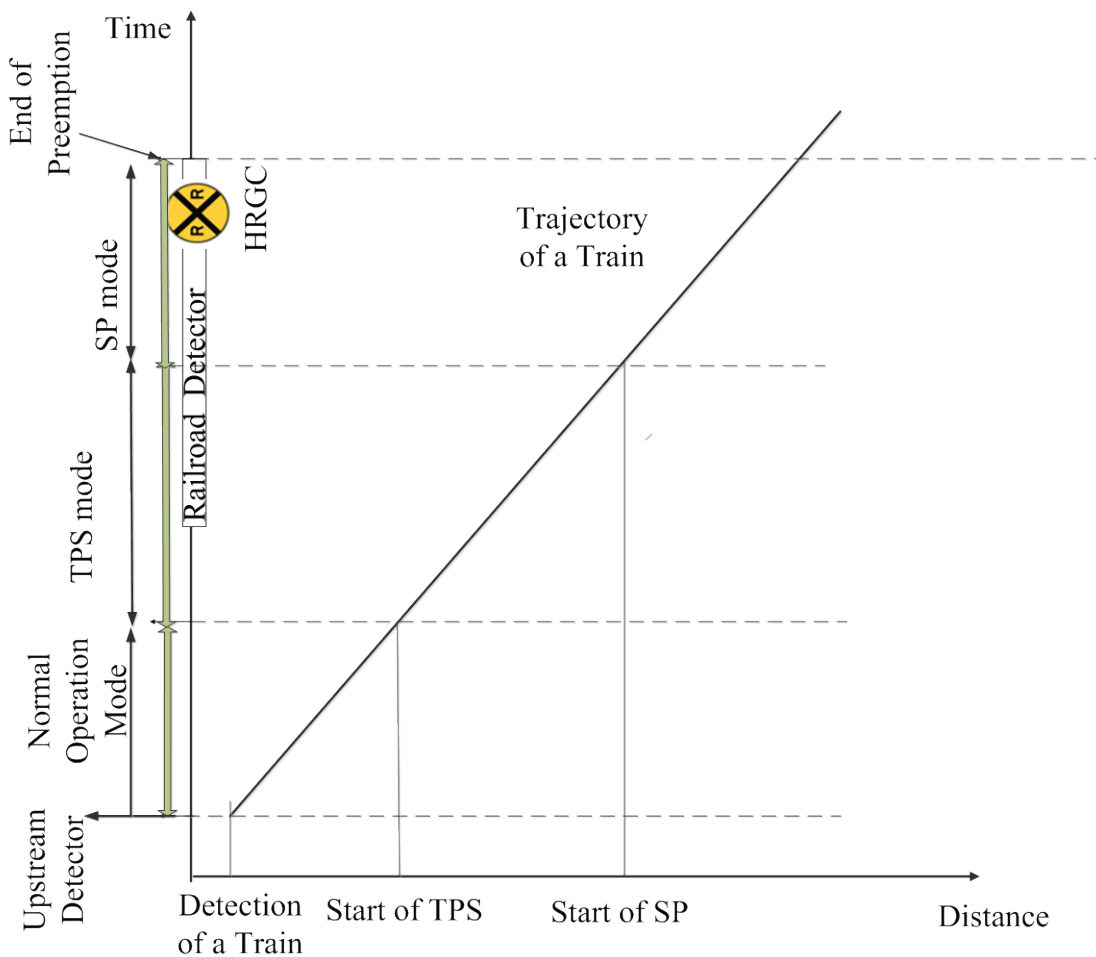
Figure 6.4 Time-distance diagram showing the relationship between TPS and SP

6.3 Limitation of the VAP Program for TPS_DT

It was found in the simulation test run that there are three specific circumstances under which the TPS_DT module cannot be initiated when it should be due to a limitation of the VAP program.

In case A of Figure 6.5, train 2 is detected by the upstream detector at location A, but has passed the position for starting the TPS_DT module. This is while train 1 is still passing through the HRGC, having cleared the HRGC detection zone, and before train 3 and train 4 have reached the positions for starting the TPS_DT algorithm. Note that these positions are dependent on train speed. In case A, the condition C3 in Figure 6.5 cannot be satisfied, thus the TPS_DT module cannot be initiated for train 2 in this case. However, the railroad standard preemption will still be initiated for train 2 after it has been detected by the railroad CWT detectors.

In case B, train 3 and train 4 pass the start points of TPS_DT before train 1 and train 2 clear the HRGC. The condition C3 in Figure 6.5 cannot be satisfied, thus the TPS_DT module cannot be initiated for both train 3 and train 4 in this case. However, the railroad standard preemption will still start after train 3 and train 4 have been detected by the railroad CWT detectors.

In case A and B, the limitation of the VAP logic is that the logic does not return to restart the TPS_DT module once all upstream trains have passed the points to start the TPS_DT module.
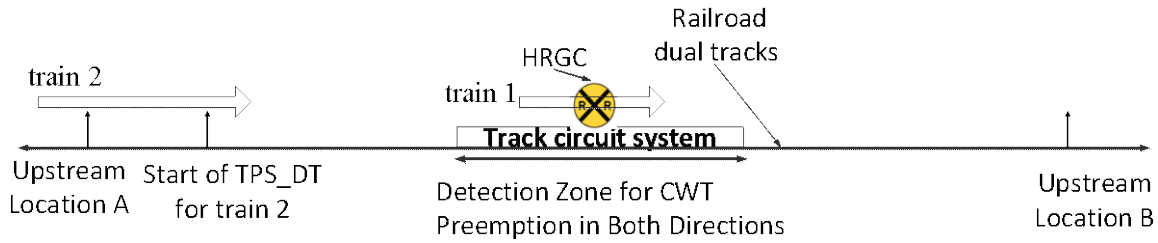
a) Case A: TPS_DT cannot start for two trains in one direction
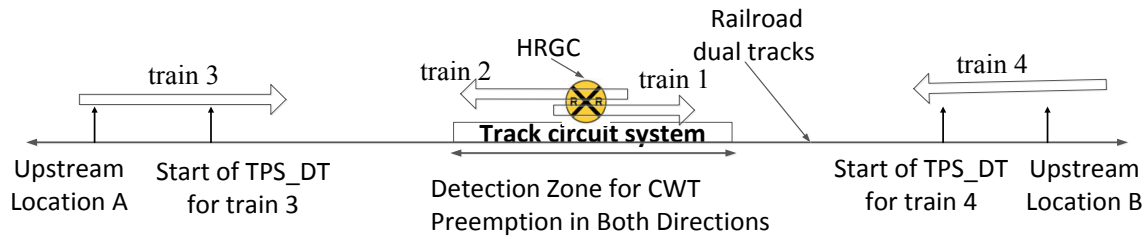
b) Case B: TPS_DT cannot start for multiple trains in both directions

Figure 6.5 Two cases in which the TPS_DT module cannot start

The third example of limitations in the VAP logic is illustrated in Figure 6.6. Train 2 is

shorter and faster than train 1, and the upstream detector at location B is closer to the railroad

circuit detector than the upstream detector at location A. Consequently, Case C_1 shows that

train 2 reaches the point that starts the TPS_DT module before train 1. In this situation, the

TPS_DT module is implemented for train 2. After train 2 enters the railroad detection zone, the

logic exits the TPS_DT module and starts the standard preemption modules for train 2. During

this period, train 1 is still being detected by the detector at upstream location A. In Case C_2,

train 2 is passing through the crossing while train 1 is still passing through upstream location A,

however, train 1 has passed the position that starts the TPS_DT module.

In this situation, the TPS_DT module will not be initiated for train 1 due to the same

limitation that the TPS_DT module cannot be started once all trains at the upstream locations

27

have passed the points that start the TPS_DT module. Note that the standard preemption will be still initiated for train 1 after it enters the detection zone.

It should be noted that the limitations of the VAP logic will result in no less pedestrian safety at the intersection near the HRGC compared to the current CWT logic because the SP will be always initiated. That is, the TPS_DT algorithm will not replace the SP, and will be as safe and efficient as the current system.

a)   Case C_1 TPS_DT is in progress for train 2

b) Case C_2 TPS_DT cannot be initiated for train 1
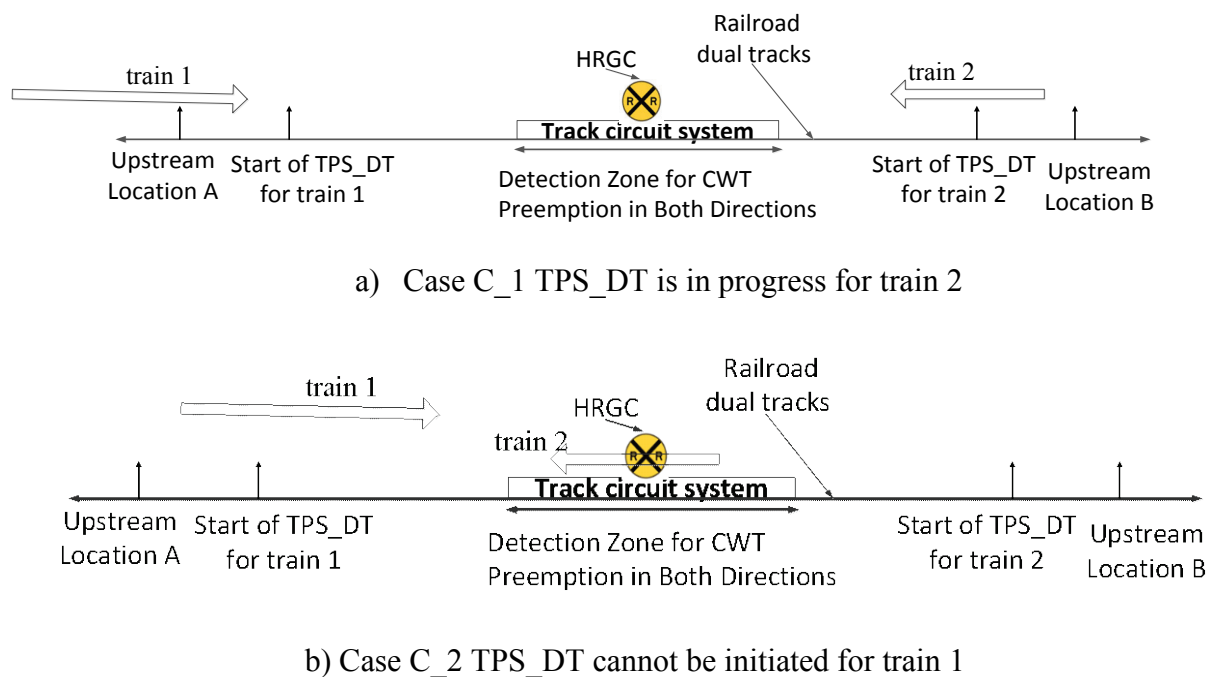
Figure 6.6 The case in which TPS_DT cannot be initiated for one of the trains in both directions

Chapter 7 Developing a GA-based Optimization Program for Signal Optimization

In this chapter, a GA-based program is developed for the optimization of traffic signals on highway-railway corridors. Subsequently, this algorithm will be tested on the test corridor.

7.1 Architecture of the GA-based Program for Signal Timing Optimization

The implementation of GA for signal timing optimization is a combination of Matlab and Visual Basic (VB) coding. The program consists of three components: the Matlab code, the VB code, and the VISSIM simulator. VISSIM is used as the simulator for the evaluation of signal timing solutions during the optimization. The Matlab code carries out the GA routines, including the generation of the initial population, the selection of parent members, crossover, elitism, and mutation. The task of the VB program is to copy candidate signal timing plans generated from the GA routines and apply them in the simulation by updating the signal timing parameters of the VISSIM model. These parameters include cycle length, split, and offset. The VB program is also connected with VISSIM through the VISSIM COM server (22). This enables the VB program to conduct multiple VISSIM simulations with the signal timing settings generated from the GA and to read simulation outputs from VISSIM. Finally, the VB program calculates fitness values of individual signal timing plans based on the simulation outputs, and sends it back to the Matlab program. Based on the fitness values, the next generation of signal timing plans is produced through the GA routine. As the program goes through continuous iterations, the algorithm will stop when the stopping criterion, which is the maximum number of runs for this research project, is met. The "best" solution is identified at this point. Note that the optimization in the program is a stochastic signal timing optimization with different random seeds.

7.2 Decision Variables for Optimization

The goal of the optimization is to improve the safety and efficiency of the signal timing operation of a highway-railroad corridor before, during, and after preemption events. Therefore,

the decision variables that are optimized should include not only the basic signal timing parameters, but also preemption-related parameters.

The basic parameters for normal signal operation are: cycle length, phase split, phase sequence, and offset. All four parameters can be optimized simultaneously using GA (23). For the optimization of signal timings during the preemption process, the phase sequence is usually kept fixed because a change of phase sequence during the preemption will make the process more complicated and, more importantly, increase the likelihood of confusion by drivers. Therefore, cycle length, phase split, and offset are chosen as the basic signal timing parameters to be optimized in the GA. For coordinated-actuated signal control, the phase split is equal to the maximum green time plus yellow and all-red intervals. Because the yellow and all-red intervals are fixed, maximum green time is actually used in GA. The force off points and permissive periods for coordination operation are calculated once the maximum green times of all phases are determined (24).

The number of preemption parameters vary for each preemption sequence. For the proposed transition preemption strategy in chapter 6, the preemption sequence is divided into four stages: (1) advance warning stage, which begins upon detection of a train by the advanced detector to the start of standard preemption by the CWT detector; (2) track clearance phase stage, which lasts from the time a train is detected by the CWT railroad detector until the train arrives at the crossing; (3) preemption dwell stage, which lasts from gate closure (gate down) to gate opening (gate up); and (4) restoring stage, which lasts from gate opening to normal operation

7.3 Objective Function and Constraints for Signal Optimization

In order to meet the safety objectives outlined in this report, the pedestrian phase truncations at conflicting pedestrian phases should be minimized and, ideally, eliminated. Consequently, a key safety measurement of effectiveness (MOE) is the number of pedestrian

30

phase cutoffs during preemption. The other safety factor is the preemption trap, which is caused by terminating the track clearance phase prior to the start of the warning lights. For this objective, the MOE is the number of track clearance phases that are terminated earlier than the start of the warning lights. The two MOEs are not incorporated into the objective function of the GA optimization because they are already considered when developing the TPS_DT algorithm in chapter 6. Nevertheless, the evaluation of the optimization results in chapter 8 will include the two MOEs as safety measures.

The target intersections that are involved in the optimization are the three intersections near HRGCs along the Cornhusker Highway corridor: 33rd St and Cornhusker Highway, 35th St and Cornhusker Highway, and 44th St and Cornhusker Highway. Their signal timings were kept fixed in the optimization. The reasons lie in that: 1) these intersections do not intersect with the BNSF railroad, and 2) do not have preemption operations, although they have the same cycle length as the target intersections. In the optimization, the three target intersections were treated as a sub-group of intersections.

The number of fractional variables used for a given intersection are a function of: 1) the signal timing plan for the intersection and 2) the optimization goals. For the three target intersections, the phase sequence is fixed during the preemption. Therefore, f_8 is not included in the vector of fractional variables. Because the target intersections have actuated-coordinated signal control, one common cycle length C is used for all the intersections along the corridor ($C = C_1 = C_2 = C_3$). In the optimization program, the fractional variable f_1 represents the common cycle length of the target intersections.

The intersection of 33rd Street and Cornhusker Highway has phases 1, 2, and 4 on the first phase ring and phases 5, 6, and 8 on the second phase ring. There is no overlap between the ring

1 and ring 2 phases, which means that phase 1 and phase 5 have the same split. Therefore, the fractional variables f_2, f_3, and f_7 are needed for this intersection, and are denoted as f_{2_33}, f_{3_33}, and f_{7_33} respectively.

The intersection of 35th Street and Cornhusker Highway has phases 2, 4, and 8 on the first phase ring, and phase 6 on the second phase ring. The fractional variables f_2, f_5, and f_7 are required for this intersection, and are written as f_{2_35}, f_{5_35}, and f_{7_35}, respectively.

The intersection of 44th St and Cornhusker Highway has phase 2 and phase 4 on the first phase ring and phases 6 and 8 on the second phase ring. Therefore, f_2 and f_7 are needed for this intersection, and are written as f_{2_44} and f_{7_44}, respectively. Table 7.1 lists all of the basic signal timing parameters for the three intersections, the fractional variables and equations to calculate them, and number of genes used to encode the variables. The agents for cycle length contain five genes, which results in a searching increment of one second based on its range of 90 s to 120 s. Note that the searching increments for the other fractional variables are not fixed because they are inter-correlated due to the constraints of the NEMA dual-ring structure, and are dependent not only on minimum/maximum splits, but also on selected cycle lengths. Therefore, these search increment value can change during each iteration of the GA process.

Table 7.1 Basic signal timing parameters and fractional variables

Intersection	Parameter	Fractional variables	Equation	# of Genes
All three intersections	cycle length	f_1	7-16	5
Intersection of 33rd St and Cornhusker Highway	(phase1+phase2)/(phase5+phase6)*, phase4/phase8	f_{2_33}	7-17/ 7-18	5
	phase1, phase2	f_{3_33}	7-19/ 7-20	5
	offset	f_{7_33}	7-35	6
Intersection of 35th St and Cornhusker Highway	phase2, (phase4+phase8)	f_{2_35}	7-17/ 7-18	5
	phase4, phase8	f_{5_35}	7-23/ 7-24	5
	offset	f_{7_35}	7-35	6
Intersection of 44th St and Cornhusker Highway	phase2/phase6, phase4/phase8	f_{2_44}	7-17/ 7-18	5
	offset	f_{7_44}	7-35	6

*This means that the sum of phase 1 and phase 2 splits are equal to that of phase 5 and phase 6 splits, while phase 4 split is equal to phase 8 split. They are calculated with f_{2_33} through Equation 7-17 and Equation 7-18.

7.3.1 Reliability and Repeatability of GA

As a global optimizer, GA can find the optimal or near-optimal solutions through its four processes of stochastic nature: generation of initial population, the reproduction process, the crossover process, and the mutation process (23). To account for the stochastic nature of traffic in the simulation models, a different random seed is used for each simulation run in GA, which again adds to the stochastic variations of the results. Park (23) has investigated the impact of random seeds on the results of a GA run and found that a GA-based program with different random number seeds will yield slightly different signal timing plans. However, the solutions will converge and GA will find at least near-optimal solutions (23). This also indicates that there

are multiple near-optimal solutions that depend on the traffic patterns and the initial GA

population. Different random seeds are used for each simulation run to ensure that the solutions

that tend to perform better under different traffic generation patterns and train speeds can survive

in the next generation (25).

Chapter 8 Sensitivity Analysis of the Methodology

In this chapter, a sensitivity analysis is conducted. It applies the GA-based signal optimization algorithm to identify the benefits of the algorithm. The process is repeated for different train demand levels.

8.1 Simulation Setup

As part of the simulation model calibration process, the empirical train speed and length distributions are incorporated in the VISSIM model. A simulation plan is set up for the sensitivity analysis. Based on the train volume data collected from the test bed, different combinations of train volume and train direction are included in the sensitivity analysis. The train demand levels are based on observations in the test bed.

8.1.1 Simulation Design

Three train volumes were chosen for use, i.e. 1 train/h, 3 trains/h, and 5 trains/h, in the sensitivity analysis. Although train volumes of 5 trains or more per hour for one direction were not observed, a sensitivity analysis on signal timings under 5 trains/h was also conducted.

The simulation time for the simulation analysis was chosen to be 3600 seconds to simulate the peak hour traffic. In each scenario, the train departure times were fixed so that a comparison between baseline and optimization scenarios could be performed under the same traffic conditions. The other advantage of fixed train departure time is that the first train can be guaranteed to enter the network right after the warm-up time of 600 s, and the analysis period is clearly defined. For the scenarios with 1 train/h, the train departs at 1800 s, which is in the middle of the simulation period. For the scenarios with 3 trains/h and 5 trains/h, the first train departs at 600 s and the last train departs at 3000 s. The intervals between two consecutive trains are 600 s and 1200 s for 3 trains/h and 5 trains/h, respectively. Based on the train departure times, an identical analysis period from 600 s to 3300 s is used for all scenarios.

Based on the combinations of two train directions and three directional train volumes, nine simulation scenarios were studied as part of the sensitivity analysis. Table 8.1b lists the nine optimization scenarios in which the proposed TPS_DT algorithm was applied. The signal timing was optimized using the GA-based program developed in chapter 7. Table 8.1a lists the nine baseline scenarios to be compared with the nine optimization scenarios in Table 8.1b. In the baseline scenarios, the current signal timing and CWT preemption logic were used.

Each scenario is labeled in the form of an "x-y-z" nomenclature. In this nomenclature "x" represents the optimization/baseline scenarios, where 1 represents an optimization scenario and 0 is a baseline scenario. The "y" parameter represents the train direction, where E represents an EB train, W represents a WB train, and B represents trains from both directions. The parameter "z" represents the number of the trains in each direction, where z is set equal to 1, 3, or 5 trains/h.

Table 8.1 Simulation Scenarios

a) Baseline Scenarios

| | | Train Volume (train/h/direction) | | |
		1	3	5
Train Direction	EB	0-E-1	0-E-3	0-E-5
	WB	0-W-1	0-W-3	0-W-5
	Both	0-B-1	0-B-3	0-B-5

b) Optimization Scenarios

| | | Train Volume (train/h/direction) | | |
		1	3	5
Train Direction	EB	1-E-1	1-E-3	1-E-5
	WB	1-W-1	1-W-3	1-W-5
	Both	1-B-1	1-B-3	1-B-5

For all scenarios, the pedestrian phases were set to be active in every cycle to assess the impact of the proposed TPS on pedestrian safety. It was assumed that pedestrians randomly arrive at the crosswalk and the arrival probabilities are subject to a negative exponential distribution. The pedestrian arriving by the end of the pedestrian clearance phase or during the current pedestrian red phase cannot make it across the intersection within the current cycle time, however, they will be allowed to actuate the next pedestrian green phase and cross the intersection. Therefore, within a cycle, the time period during which a pedestrian could enter the next pedestrian phase is that from the time the pedestrian green phases are terminated to the end of the cycle.

Based on this, the probability of the pedestrian phase being active during every cycle is equal to the probability of more than one pedestrian arriving at the intersection within the cycle time, after the pedestrian green phase of that cycle ends. For the test corridor, the shortest pedestrian green phase is 5 s and the longest possible cycle length is 120 s. Therefore, the length of the time period during which pedestrians can stop at a pedestrian cross walk and enter the next pedestrian phase is 115 s.

Because the pedestrian phases are active in every cycle, the probability of a pedestrian phase being truncated upon start of the track clearance phase can be as high as 99.9 percent for the current CWT system. It has been proven that the newly developed transition preemption strategies (i.e. TPS2 and TPS3) (8) can decrease or eliminate the pedestrian phase cutoffs. It is hypothesized that the proposed TPS_DT in this report will also decrease or eliminate the pedestrian phase truncations at the intersections near the HRGCs under current CWT preemption operation.

8.2 Optimization Results of One Hour Simulation Scenarios

8.2.1 Optimized Signal Timing Settings

The GA-based program developed in chapter 7 was used to identify the "best" signal

timing parameter set for each simulation scenario shown in Table 8.1b. Six intersections along

Cornhusker Highway (i.e. the intersection of 27th St and Cornhusker Highway, 29th St and

Cornhusker Highway, 33rd St and Cornhusker Highway, 35th St and Cornhusker Highway, 44th

St Cornhusker Highway, and 48th St and Cornhusker Highway) are involved in calculating the

fitness value. For each scenario, the program generated a total of 900 (30 individuals per

generation × 30 generations) signal timing plans and evaluated them in 900 simulation runs. It

took the optimization program approximately 40 hours to complete the 900 simulation runs,

using a computer equipped with an Intel Core i7 3.60 GHz processor and 16.0 GB of memory.

Figure 8.1 shows the convergence curve of the GA results for scenario 1-B-5 with 5

trains in both directions. This was chosen to illustrate the process because this is the scenario

with the heaviest train traffic. It can be seen that the minimum corridor delay for each generation

tends to decrease as the number of generations increases. Note that there is some variability in

the fitness value corridor delay, in that while the general trend is downward, some iterations

actually result in an increase in corridor delay. This is due to the randomness in the simulation

settings, such as random seed and train/vehicle speed distribution. In addition, the best fitness

value was 75 s/veh in the 25th generation of GA.
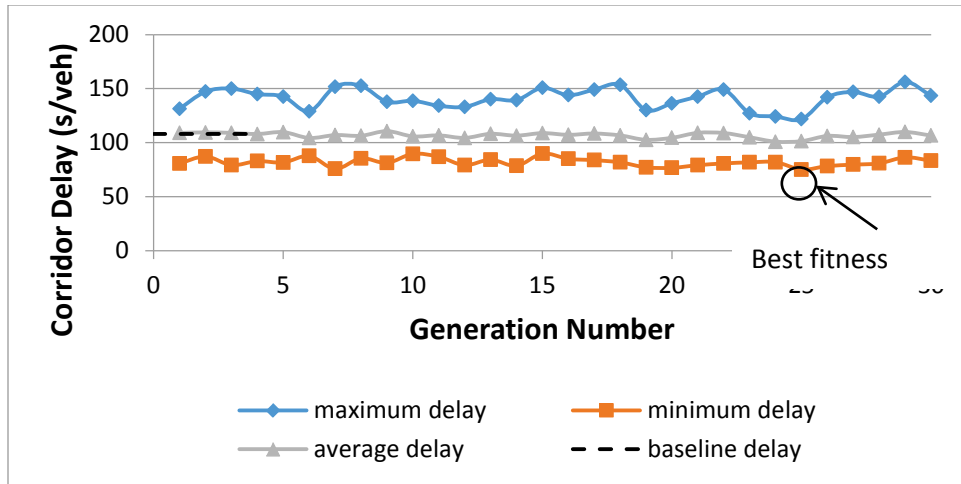
Figure 8.1 Minimum generation fitness value vs. generation number in scenario 1-B-5

The optimized cycle length ranges from 91 s to 117 s, with an average of 103 s. On average, the optimization assigns more than double the green time to the left-turn phases (phase 1 and phase 5) of the signal at 33rd St intersection, 6 percent more green time to phase 8 of the signal at 35th St intersection, and about 32 percent more green time to phase 4 and phase 8 of the signal at the 44th St intersection, as compared to the baseline signal timings. Note that phase 5, phase 4, and phase 8 are the phases that conflict with the train and are blocked during the dwell stage of preemption. Assigning more green time to these phases will probably help reduce the queuing vehicles during preemption. More green time is also assigned to the track clearance phase and exit phase of the three target intersections. This strategy helps clear more vehicles off the conflicting approaches a) shortly before the train arrives at the crossings, and b) immediately after the train departs the crossings. Finally, it was found that the average advanced preemption warning time (APWT) varies from 84 seconds to 102 seconds for the EB direction and from 51 seconds to 84 seconds for the WB direction.

39

8.2.2 Evaluation with Optimized Signal Timing Plans

After the optimization process is finished, an evaluation of the optimized signal timing plans is conducted. For the evaluation of safety, the number of pedestrian phase cutoffs and the number of preemption traps at each intersection near a HRGC were used as the measures of effectiveness (MOEs). For the evaluation of traffic efficiency, three MOEs were used: 1) the average delay of the three object intersections near HRGCs, 2) the average delay of the six intersections on the Cornhusker Highway corridor, which represents the corridor performance, and 3) the average delay of the whole study network, which represents the network performance. The purpose is to evaluate the impact of the optimized signal timings at three different levels.

To control the stochastic variability in the VISSIM simulation, 50 multiple random-seeded simulation runs are performed with the optimized signal timings from the nine optimization scenarios. Another 50 multiple simulation runs with the same set of random seeds were performed for the respective nine baseline scenarios with the current signal timing plan. This ensures that traffic patterns and train characteristics were identical for each optimization scenario and its corresponding baseline scenario. A VB-based program was developed and used to conduct multiple simulation runs and obtain the MOE values from VISSIM. The next section discusses the evaluation results of pedestrian safety and delay.

8.2.2.1 Evaluation of Pedestrian Phase Truncations

8.2.2.1.1 Pedestrian Phases for Safety Evaluation

For the study corridor, the pedestrian phase corresponding to the coordinated phases on Cornhusker Highway (P2 and P6), and the pedestrian phase on the southbound competing approach that is perpendicular to the railroad tracks (P8), were analyzed as part of the safety evaluation. Two conditions of pedestrian phase truncation were considered.

Figure 8.2 shows the first condition, where the pedestrian phases with the main phases on Cornhusker Highway (P2 and P6) are truncated by the track clearance phase (phase 4). A typical example of this condition in the simulation is shown in Figure 8.3. Here the pedestrians crossing 44th Street in the E-W direction were "stranded" in the intersection and in potential conflict with NB vehicles that are part of the track clearance phase.
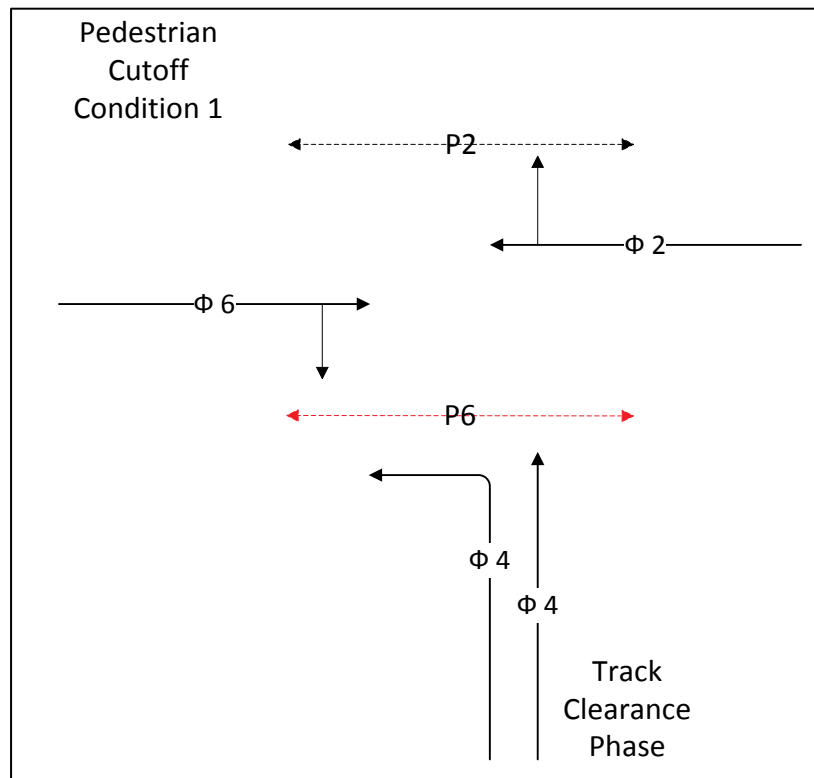
Figure 8.2 Condition I of pedestrian phase truncation
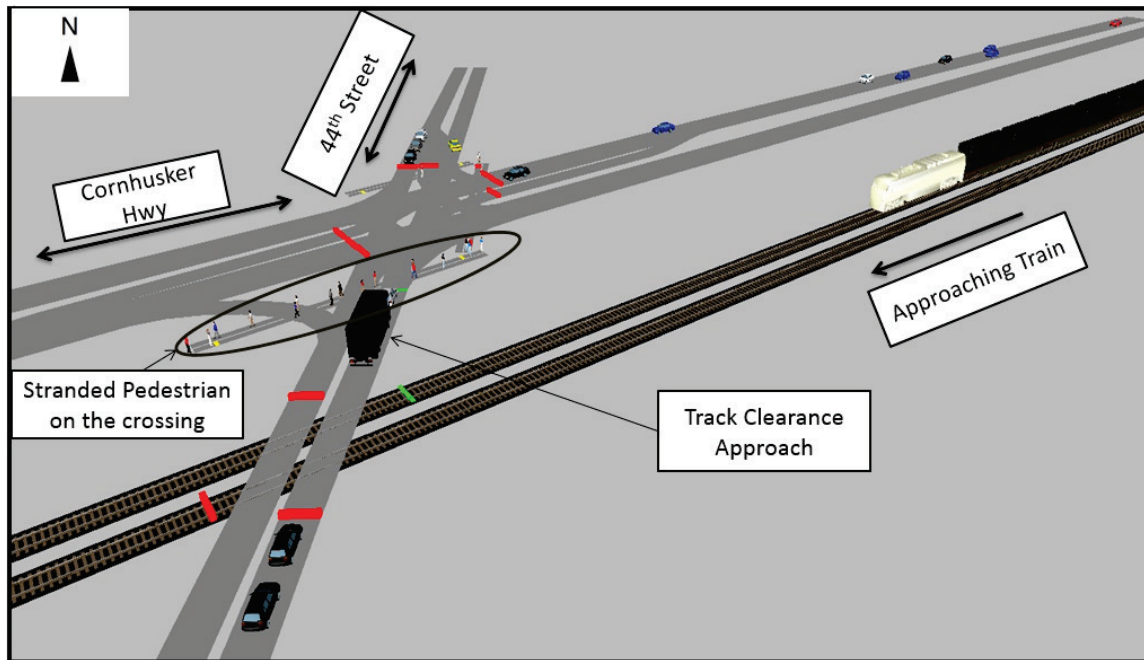
Figure 8.3 Simulation example of pedestrian phase truncation for Condition I
(Note that the EB-WB pedestrian phase was abruptly truncated and pedestrians are in conflict
with the NB vehicle that has been given time to clear the tracks)

Figure 8.4 shows the second condition of the pedestrian phase cutoff, which has phase 8

in conflict with the left-turn movement of the track clearance phase. It is also considered unsafe

during track clearance, although the left-turn movement is permissive with phase 8 in the normal

operation mode. Note that the conflict between phase 4 and the right-turn movement of the track

clearance phase is considered safe, because right-turn vehicles are supposed to yield to

pedestrians crossing the intersection. Therefore, the truncation of phase 4 is not considered as

part of the safety evaluation.
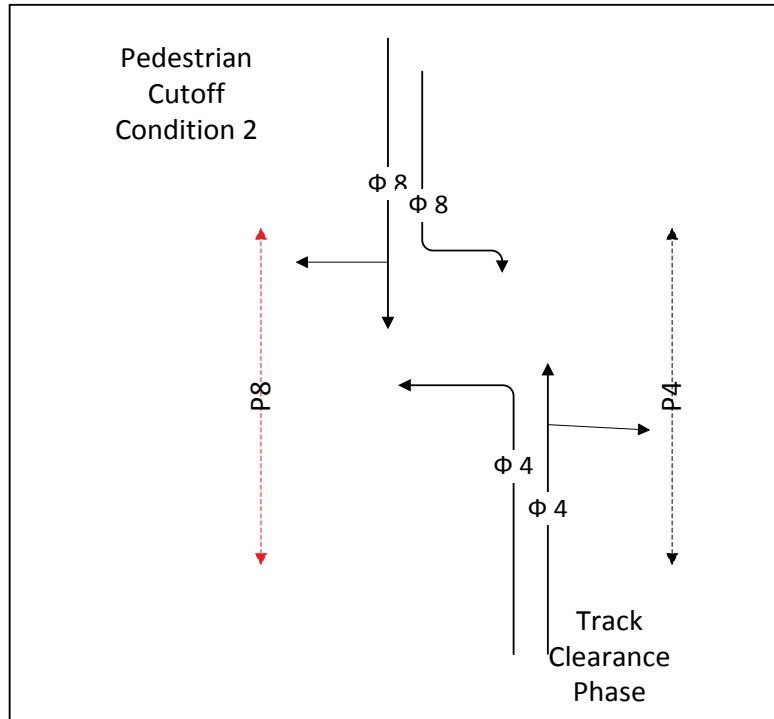
Figure 8.4 Condition II of pedestrian phase truncation

In the VAP code of signal timings for the three intersections, the parameter "cutoff" was defined to count the number of pedestrian phase cutoffs upon the start of the preemption. The parameter "count" was used to count the number of preemptions once a preemption event ends. It should be noted that the number of preemption events at a HRGC can be equal or less than the number of trains passing the HRGC, because in the case of two simultaneous trains passing one HRGC, there is only one preemption sequence occurring instead of two.

8.2.2.1.2 Evaluation Results

Reductions in the percentages of pedestrian phase cutoffs in the optimization scenarios ranged from 59 percent to 100 percent, compared to their baseline scenarios. In the scenarios with one train (scenario 1-E-1, scenario 1-W-1), the pedestrian truncation has been eliminated, because the TPS_DT module were initiated for every preemption event in these scenarios. For the other scenarios, it was observed that more than one train passed the HRGCs during the

simulation, and the TPS_DT module could not be initiated for all the preemption events due to the limitations of the VAP logic for TPS_DT discussed in section 6.3. This resulted in pedestrian phase cutoffs as only the CWT preemptions were initiated. The limitations of the VAP logic can be addressed in the later implementation, and it is hypothesized that the pedestrian phase cutoffs in all the scenarios would be eliminated.

8.2.2.2 Evaluation of Preemption Trap

The preemption trap will not occur in the standard preemption (SP), because the track clearance phase and the flashing of the warning lights start simultaneously. The TPS_DT algorithm operates between the end of the normal operation and the start of the SP. Even if there were considerable errors associated with predicted train arrival time, the SP will not begin earlier than the expected. Therefore, it is hypothesized that the TPS_DT algorithm will not cause any preemption traps.

8.2.2.3 Evaluation of Delay Improvement

8.2.2.3.1 Comparison between Baseline Scenarios with Current Signal Timing and Optimization Scenarios with TPS_DT

As discussed at the beginning of this chapter, the three MOEs for delay evaluation (average delay of the three intersections near HRGCs, average delay of the whole corridor, and network delay) from 50 random-seeded simulations were obtained through the VB-based program. The mean and standard deviation (std) of the MOEs were also calculated, and a one-tail paired t-test was applied to compare the MOEs of the optimization scenarios with those of the respective baseline scenarios. The paired t-test is appropriate because the only difference in the simulation runs was the inclusion of the new preemption logic.

It can be seen in Table 8.2 and Table 8.3 that all optimized signal solutions result in a decrease of delay on the three target intersections and the whole corridor. There were statistically significant improvements on the average delay of the three target intersections at the 5 percent significance level in eight of the nine scenarios. The only exception was scenario 1-W-3. On average, there is a 14.3 percent reduction in average delay and a 24.2 percent reduction of its standard deviations for the nine scenarios. Note that a lower value of standard deviations of delay indicate that the optimized signal timings result in more consistent delay than the current timings. At the corridor level (Table 8.3), there are significant decreases in corridor delay in the nine scenarios at a 95 percent confidence level. Over the nine scenarios, there is a 10.2 percent decrease in average corridor delay and a 4.4 percent decrease of its standard deviation. As shown in Table 8.4, the average network delays for the optimization scenarios are significantly higher than those of the respective baseline scenarios. On average, there is a 5 percent increase in average network delay, and a 7 percent increase in the standard deviation of network delay.

The improvement of delay for the three intersections near HRGCs is higher than that for the whole corridor. This is probably because the signal timing settings of the other three intersections in the corridor (27th St and Cornhusker Highway, 29th St and Cornhusker Highway, and 48th St and Cornhusker Highway) were not optimized, and this averaged out the improvement at the three intersections near HRGCs. In addition, the optimization leads to increased average network delay, which indicates that there is a tradeoff between improving corridor performance and network performance. It could be argued that during preemption events the corridor traffic is more important than the whole network, and more weight should be placed on improving safety and traffic flow of the corridor with HRGCs. Alternatively, the optimization could be conducted with the objective of minimizing average network delay.

Table 8.2 Comparison of multiple run results between optimization and baseline scenarios: average delay of the three target intersections near HRGCs

Number of Trains	Scenarios	(1) Average baseline	(2) Average optimized	$\dfrac{(2) - (1)}{(1)}$	(3) STD baseline	(4) STD optimized	$\dfrac{(4) - (3)}{(3)}$	P(T<=t)	H_0*: (1)=(2) H_A: (1)>(2)
1 Train in EB	Scenario 0-E-1 vs Scenario 1-E-1	60.27	48.30	-19.9%	14.85	7.77	-47.7%	0.00	Reject H_0
3 Trains in EB	Scenario 0-E-3 vs Scenario 1-E-3	66.93	61.82	-7.6%	17.37	13.44	-22.6%	0.01	Reject H_0
5 Trains in EB	Scenario 0-E-5 vs Scenario 1-E-5	89.96	76.48	-15.0%	28.23	23.87	-15.4%	0.00	Reject H_0
1 Train in WB	Scenario 0-W-1 vs Sscenario 1-W-1	62.73	51.86	-17.3%	15.35	9.07	-40.9%	0.00	Reject H_0
3 Trains in WB	Scenario 0-W-3 vs Scenario 1-W-3	71.10	68.46	-3.7%	18.17	15.15	-16.6%	0.07	Accept H_0
5 Trains in WB	Scenario 0-W-5 vs Scenario 1-W-5	96.91	83.50	-13.8%	28.49	20.31	-28.7%	0.00	Reject H_0
1 Train in EB & WB	Scenario 0-B-1 vs Scenario 1-B-1	68.28	57.27	-16.1%	15.93	11.42	-28.3%	0.00	Reject H_0
3 Trains in EB &WB	Scenario 0-B-3 vs Scenario 1-B-3	69.30	57.23	-17.4%	16.36	10.69	-34.7%	0.00	Reject H_0
5 Trains in EB &WB	Scenario 0-B-5 vs Scenario 1-B-5	129.67	108.29	-16.5%	49.23	42.85	-13.0%	0.00	Reject H_0
Average		79.46	68.14	**-14.3%**	22.66	17.17	-24.2%		

* Reject H_0 at the 5% significance level

Table 8.3 Comparison of multiple run results between optimization and baseline scenarios: average corridor delay

Number of Trains	Scenarios	(1) Average baseline	(2) Average optimized	$\frac{(2)-(1)}{(1)}$	(3) STD baseline	(4) STD optimized	$\frac{(4)-(3)}{(3)}$	P(T<=t)	H_0*: (1)=(2) H_1: (1)>(2)
1 Train in EB	Scenario 0-E-1 vs Scenario 1-E-1	72.57	65.12	-10.3%	5.23	4.68	-10.5%	0.00	Reject H_0
3 Trains in EB	Scenario 0-E-3 vs Scenario 1-E-3	77.27	73.60	-4.8%	6.35	6.20	-2.3%	0.00	Reject H_0
5 Trains in EB	Scenario 0-E-5 vs Scenario 1-E-5	88.41	85.15	-3.7%	9.11	10.33	13.4%	0.00	Reject H_0
1 Train in WB	Scenario 0-W-1 vs Sscenario 1-W-1	74.77	69.90	-6.5%	5.02	4.28	-14.7%	0.00	Reject H_0
3 Trains in WB	Scenario 0-W-3 vs Scenario 1-W-3	77.95	75.52	-3.1%	5.82	6.43	10.5%	0.00	Reject H_0
5 Trains in WB	Scenario 0-W-5 vs Scenario 1-W-5	91.46	84.59	-7.5%	7.98	8.59	7.6%	0.00	Reject H_0
1 Train in EB & WB	Scenario 0-B-1 vs Scenario 1-B-1	77.26	66.30	-14.2%	6.43	5.37	-16.5%	0.00	Reject H_0
3 Trains in EB &WB	Scenario 0-B-3 vs Scenario 1-B-3	86.12	70.56	-18.1%	7.91	5.42	-31.5%	0.00	Reject H_0
5 Trains in EB &WB	Scenario 0-B-5 vs Scenario 1-B-5	108.05	86.42	-20.0%	14.83	14.36	-3.2%	0.00	Reject H_0
Average		83.76	75.24	-10.2%	7.63	7.30	-4.4%		

* Reject H_0 at the 5% significance level

Table 8.4 Comparison of multiple run results between optimization and baseline scenarios: average network delay

Number of Trains	Scenarios	(1) Average baseline	(2) Average optimized	$\frac{(2)-(1)}{(1)}$	(3) STD baseline	(4) STD optimized	$\frac{(4)-(3)}{(3)}$	P(T<=t)	H_0*: (1)=(2) H_1: (1)<(2)
1 Train in EB	Scenario 0-E-1 vs Scenario 1-E-1	325.51	356.70	9.6%	13.83	17.54	26.9%	0.00	Reject H_0
3 Trains in EB	Scenario 0-E-3 vs Scenario 1-E-3	346.20	375.99	8.6%	18.82	21.93	16.5%	0.00	Reject H_0
5 Trains in EB	Scenario 0-E-5 vs Scenario 1-E-5	384.98	414.63	7.7%	23.81	27.56	15.7%	0.00	Reject H_0
1 Train in WB	Scenario 0-W-1 vs Sscenario 1-W-1	330.45	364.08	10.2%	13.65	14.82	8.6%	0.00	Reject H_0
3 Trains in WB	Scenario 0-W-3 vs Scenario 1-W-3	352.17	377.88	7.3%	16.24	22.36	37.7%	0.00	Reject H_0
5 Trains in WB	Scenario 0-W-5 vs Scenario 1-W-5	403.77	429.83	6.5%	21.41	24.52	14.5%	0.00	Reject H_0
1 Train in EB & WB	Scenario 0-B-1 vs Scenario 1-B-1	335.90	358.91	6.8%	19.13	18.52	-3.2%	0.00	Reject H_0
3 Trains in EB &WB	Scenario 0-B-3 vs Scenario 1-B-3	376.58	369.28	-1.9%	23.81	17.50	-26.5%	0.03	Reject H_0
5 Trains in EB &WB	Scenario 0-B-5 vs Scenario 1-B-5	472.22	450.10	-4.7%	31.29	30.07	-3.9%	0.00	Reject H_0
Average		369.75	388.60	5.1%	20.22	21.65	7.1%		

* Reject H_0 at the 5% significance level

8.2.2.3.2 Comparison between Baseline Scenarios with Optimized Signal Timings and Optimization Scenarios with TPS_DT

The previous section compared the MOEs under the current signal timing plan with the CWT preemption to the optimized signal timing plans with the TPS_DT algorithm. The algorithm results revealed a statistically significant reduction in corridor-level delay. However, it is unknown whether the reduction of delay was contributed to the optimization of the basic signal timing parameters alone (cycle length, maximum phase duration, and offset) or that of the preemption-related parameters.

In this section, the current signal timing plan with CWT preemption was optimized using the GA-based program for the three baseline scenarios that have the highest train volumes (scenario 0-E-5, scenario 0-W-5, and scenario 0-B-5). The new scenarios are denoted as scenario 2-E-5, scenario 2-W-5, and scenario 2-B-5, where "2" represents the scenarios of optimizing the basic signal timing parameters. The optimized basic signal timings were evaluated with 50 multiple simulation runs, and the results were then compared with those of the corresponding optimization scenarios, where both basic signal timing parameters and TPS-related parameters were optimized.

Tables 8.5, 8.6, and 8.7 summarize the evaluation results in the three optimization scenarios with CWT preemption and their corresponding optimization scenarios with TPS_DT. In the scenarios with 5 trains in EB, the optimized signal timings with TPS_DT did not have statistically significant reduction in the three delay MOEs as compared to the optimized signal timings with CWT preemption. However, in the scenarios with 5 trains in WB and 5 trains in both directions, the optimized signal timings with TPS_DT resulted in a statistically significant lower average delay for both the target intersections and the corridor, compared to the optimized

49

signal timings with CWT preemption. This indicates that in general the proposed methodology with the TPS_DT algorithm and simultaneous optimization of both basic signal timing parameters and preemption-related parameters did a better job in reducing the corridor-level delay, even when compared to the methodology with the CWT preemption and optimization of only basic signal timing parameters.

Table 8.5 Comparison of multiple run results between optimization scenarios with TPS_DT and optimization scenarios with basic signal timings: average delay of the three target intersections near HRGCs

Number of Trains	Scenarios	(1) Average Optimized (CWT)	(2) Average Optimized (TPS_DT)	$\frac{(2)-(1)}{(1)}$	(3) STD baseline	(4) STD optimized	$\frac{(4)-(3)}{(3)}$	P(T<=t)	H_0*: (1)=(2) H_1: (1)≠(2)
5 Trains in EB	Scenario 2-E-5 vs Scenario 1-E-5	74.37	76.48	2.84%	69.36	69.59	0.33%	0.15	Accept H_0
5 Trains in WB	Scenario 2-W-5 vs Scenario 1-W-5	94.09	83.50	-11.26%	25.10	20.31	-19.09%	0.00	Reject H_0
5 Trains in EB & WB	Scenario 2-B-5 vs Scenario 1-B-5	114.72	108.29	-5.60%	47.19	42.85	-9.19%	0.015	Reject H_0

* Reject H_0 at the 5% significance level

Table 8.6 Comparison of multiple run results between optimization scenarios with TPS_DT and optimization scenarios with basic signal timings: average corridor delay

Number of Trains	Scenarios	(1) Average Optimized(CWT)	(2) Average Optimized(TPS_DT)	$\frac{(2)-(1)}{(1)}$	(3) STD baseline	(4) STD optimized	$\frac{(4)-(3)}{(3)}$	P(T<=t)	H_0*: (1)=(2) H_1: (1)≠(2)
5 Trains in EB	Scenario 2-E-5 vs Scenario 1-E-5	86.46	85.15	-1.51%	10.75	10.33	-3.88%	0.17	Accept H_0
5 Trains in WB	Scenario 2-W-5 vs Scenario 1-W-5	89.65	84.59	-5.65%	9.19	8.59	-6.56%	0.00	Reject H_0
5 Trains in EB & WB	Scenario 2-B-5 vs Scenario 1-B-5	103.72	86.42	-16.67%	13.80	14.36	4.04%	0.00	Reject H_0

* Reject H_0 at the 5% significance level

Table 8.7 Comparison of multiple run results between optimization scenarios with TPS_DT and optimization scenarios with basic signal timings: average network delay

Number of Trains	Scenarios	(1) Average Optimized (CWT)	(2) Average Optimized (TPS_DT)	$\frac{(2)-(1)}{(1)}$	(3) STD baseline	(4) STD optimized	$\frac{(4)-(3)}{(3)}$	P(T<=t)	H_0*: (1)=(2) H_1: (1)≠(2)
5 Trains in EB	Scenario 2-E-5 vs Scenario 1-E-5	414.65	414.63	0.00%	29.68	27.56	-7.15%	0.99	Accept H_0
5 Trains in WB	Scenario 2-W-5 vs Scenario 1-W-5	422.81	429.83	1.66%	24.57	24.52	-0.19%	0.035	Reject H_0
5 Trains in EB & WB	Scenario 2-B-5 vs Scenario 1-B-5	488.18	450.10	-7.80%	35.60	30.07	-15.53%	0.00	Reject H_0

* Reject H_0 at the 5% significance level

8.3 Real-time Signal Timing Optimization

The one hour signal timing optimization procedure used in the last section assumed that train volumes and departure times are fixed within the one hour, as previous research (7, 8) has done. If train speed, train length, and departure time are random, a real-time optimization is required when a train is detected at the upstream detection location.

A real-time signal timing optimization was performed for the scenario of two simultaneous trains from both directions. The simulation duration for the scenario is 1800 seconds, including a warm-up time of 600 seconds. In the simulation, the trains start at 600 seconds, with a fixed train speed of 35 km/h. Based on this speed, the trains will leave the network at approximately 1200 seconds. The analysis period was set to the period of 600 seconds to 1500 seconds, because it covers the travel time of the train when passing through the network with the specified speed. Figure 8.5 shows the analysis period for the simulation, which is 15 min in length and lasts from 600 s to 1500 s. The median of the train length distribution found from the train model parameter calibration, which is 2632 meters, was used as the train length.
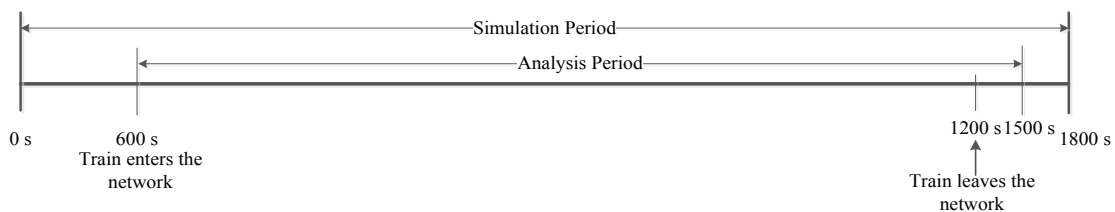
Figure 8.5 Time frame for analysis period during 1800 s simulation

It should be noted for this optimization that the GA-based optimization program needs 30 hours to finish all the simulation runs, which is too long for a real-time signal timing optimization. Considering the mean travel time of trains from the upstream location to the closest HRGC, the optimization time should not exceed 2 minutes for practical implementation. To

53

achieve this goal: 1) a parallel computation technique (26) can be applied to enhance the computation speed of GA, 2) the GA search space can be reduced, 3) the number of parameters in the optimization can be reduced, and 4) some combinations of option 1, 2, and 3 can be implemented.

Two strategies of GA optimization were tested for this scenario:

(1) Full optimization: optimizing the basic signal timing parameters and preemption-related parameters simultaneously;

(2) Partial optimization: optimizing the preemption-related parameters while maintaining the basic signal parameters from the current signal timing plan.

Table 8.8 shows the aggregated simulation results. It may be seen that the optimized signal timings from both the full optimization and the partial optimization scenarios eliminate the pedestrian phase cutoffs in this scenario. Table 8.9 and Table 8.10 show the evaluation results of 50 random-seeded multiple simulation runs for full optimization and partial optimization, respectively. In the full optimization, the average delays of the three target intersections and the whole corridor have been reduced by 11 percent and 5.8 percent, respectively. These results were statistically significant at the 95 percent level of confidence. By optimizing preemption-related parameters, the delay reduction was only 1.9 percent for the three target intersections and 1.1 percent for the corridor. Neither of these reductions were statistically significant. The average network delay was increased by 3.3 percent for the full optimization scenario and 1.0 percent for the partial optimization scenario. These increases were statistically significant at the 95 percent confidence level.

Table 8.8 Comparison of pedestrian safety results between optimized and baseline signal timings

	1 train in both directions		
33rd St Intersection	baseline	Full optimization	Partial optimization
# of Ped Cutoffs	50	0	0
# of Ped Events	50	50	50
Percentage	100.0%	0.0%	0.0%
Improvements		100.0%	100.0%
35th St Intersection	baseline	optimized	optimized
# of Ped Cutoffs	50	0	0
# of Ped Events	50	50	50
Percentage	100.0%	0.0%	0.0%
Improvements		100.0%	100.0%
44th St Intersection	baseline	optimized	optimized
# of Ped Cutoffs	0	0	0
# of Ped Events	50	50	50
Percentage	0.0%	0.0%	0.0%
Improvements		0.0%	0.0%

Table 8.9 Evaluation results for full optimization (50 multiple simulation runs)

MOEs (s/veh)	(1) Average baseline	(2) Average optimized	$\frac{(2)-(1)}{(1)}$	(3) STD baseline	(4) STD optimized	$\frac{(4)-(3)}{(3)}$	p-value H0: (1)=(2) H1: (1)≠(2)
3 Intersection Average Delay	62.05	55.15	-11.1%	8.32	5.45	-34.5%	0.00
Corridor Delay	59.04	55.63	-5.8%	3.99	2.66	-33.3%	0.00
Network Delay	217.82	225.10	3.3%	6.25	6.25	0.0%	0.00

Table 8.10 Evaluation results for partial optimization (50 multiple simulation runs)

MOEs (s/veh)	(1) Average baseline	(2) Average optimized	$\frac{(2)-(1)}{(1)}$	(3) STD baseline	(4) STD optimized	$\frac{(4)-(3)}{(3)}$	p-value H0: (1)=(2) H1: (1)≠(2)
3 Intersection Average Delay	62.05	60.90	-1.9%	8.32	8.37	0.6%	0.12
Corridor Delay	59.04	58.37	-1.1%	3.99	3.98	-0.3%	0.09
Network Delay	217.82	220.07	1.0%	6.25	7.96	27.3%	0.00

8.4 Effects of Prediction Errors on Signal Timing Optimization

In the current version of the VISSIM model, a train has constant speed throughout the network. In the VAP logic, the arrival time of a train at the HRGC is predicted as the distance from the upstream detection location to the target HRGC divided by the train speed, and it is updated simply by counting down the predicted arrival time at the upstream location. In other words, there was no prediction error for train arrivals in the previous analysis. However, prediction of real train arrivals cannot be 100 percent accurate. Therefore, it is necessary to investigate the effects of prediction errors on safety and delay of the corridor. A train arriving earlier has a negative prediction error, while a late train has a positive prediction error.

The real-time scenario with one train in both directions was used as a case study to investigate the effects of the train arrival prediction error on safety and delay. The 30-minute optimization scenario and the signal timing setting from the full optimization in the previously mentioned scenario were used for the study. All the results were based on 50 random-seeded simulation runs.

The negative prediction errors in the TPS_DT caused 34 percent to 100 percent of the pedestrian phase cutoffs. The positive prediction errors resulted in a 12 percent increase of delay at the three target intersections, and 5 percent increase of delay in the whole corridor. The pedestrian phase truncations can be eliminated by omitting the pedestrian phases at a time point earlier than the constant warning time, plus the negative prediction error time. The increase of delay due to positive prediction errors can be controlled by increasing the accuracy of the prediction models, or by correcting the prediction with the positive prediction errors.

Chapter 9 Conclusions and Future Research

9.1 Conclusions

A methodology of adaptive signal timing optimization for a corridor with multiple HRGCs was developed for this research. The methodology contains three parts: a prediction model for train arrival times, a transition preemption strategy for dual tracks (TPS_DT), and a GA-based optimization program. Based on the railroad traffic characteristics in the field, nine one-hour simulation scenarios were set up to evaluate the GA-based optimization method. The purpose of the one hour simulation scenarios were to test if the GA-based optimization program can be used for off-line optimization, given that the train speeds and departure times were known. It was found that the optimized signal timing plans with TPS_DT can significantly improve both the safety and efficiency of the corridor. In the scenarios with 5 trains/h in WB and both directions, the improvements were even considerably higher than those of the best signal timing solutions with the current CWT preemption. It was found that pedestrian signal truncations have not been eliminated in the scenarios with more than one train in a direction, because the VAP logic cannot initiate the TPS_DT module for each preemption under certain conditions of multiple trains. However, the limitation of the TPS_DT logic coded in VAP may not be an issue for a signal controller, field studies need to be conducted to check if the limitation may be avoided in the field implementation.

A real-time optimization scenario with two trains in both directions was designed to test the benefits of the proposed methodology in real-time signal timing optimization, given that a train is present at the upstream location. The optimization was performed offline. However, it could be implemented on-line and eventually become a real-time optimization.

The other factor that may cause pedestrian phase cutoffs is prediction error, specifically a train arriving earlier than predicted. On the other hand, the late arrival of a train would result in

long track clearance time, and consequently higher delay. Therefore, it is necessary to investigate the effects of prediction errors on pedestrian safety and intersection delay. In the simulation, train speed was modeled as average speed over the rail segment between the upstream location and the specified HRGC, due to the limitation of modeling instantaneous train speed in the VISSIM model. As a result, prediction error was modeled by adding an error term to the equation of predicted train arrival time in the VAP logic.

The results of the 30-minute simulation scenario showed that trains that arrived earlier started the SP earlier, which resulted in higher percentages of pedestrian truncations, while trains arriving later lead to higher corridor delay. In order to minimize the number of conflicting pedestrian phases that are truncated, the pedestrian phases can be prohibited at an earlier time point that covers the prediction error. To maintain the benefit of optimization in delay reduction, the positive prediction errors need to be controlled within 20 s. This can be achieved by enhancing the accuracy of the prediction models.

9.2 Future Research

A frame of the optimization methodology was developed, and the parts of the methodology were tested separately during this research process. For future research, some steps can be conducted to streamline the methodology. First, methods to model instantaneous train speed profiles in VISSIM need to be addressed. The second step is to incorporate appropriate prediction models (e.g. kinematic or regression models) in the VAP logic to forecast train arrival time. In the third step, a correction factor concerning the error bounds of prediction can be applied to the train arrival time prediction in the VAP logic to minimize the prediction errors.

Further, updating the data set for the regression models can enhance the accuracy of prediction; however, the update frequency of the prediction models needs to be studied. For

58

example, it is not clear whether the models should to be updated on a monthly, weekly, or continuous basis.

The research presented in this report only developed the prediction models for EB trains. Prediction models for the WB trains need to be established and incorporated in the optimization methodology. In addition, the methodology is developed based on the test corridor on Cornhusker Highway. To prove its transferability, the methodology should be tested on other test beds.

The optimization strategy focused on the corridor, meaning that only the signal timings of the three target intersections near HRGCs were optimized. The optimized signal timing resulted in an increase of network delay, although corridor delay and pedestrian safety were significantly improved. An expansion of the GA optimization to an area level, including the intersections close to the intersections on Cornhusker Highway and main intersections on 27th St and 48th Street, may alleviate this problem.

Parallel computation can be used to enhance the calculation speed of GA, and to fulfill the requirement for real-time implementation. Considering the average travel time of trains from the upstream location to the HRGC, it is hypothesized that a two minute or less computation time is appropriate for online optimization.

For this research, all simulations were performed using AM peak hour traffic volumes. The BNSF railroad section at the Cornhusker Highway corridor is operated 24 hours a day. The new transition preemption strategy TPS_DT may have a different performance under different traffic volumes. Therefore, it is necessary to investigate the benefits of the optimization methodology under different traffic demand levels (e.g. medium and low traffic demand levels).

The VAP logic with TPS_DT was developed and tested in a simulation environment. To implement the logic in the field, hardware-in-the-loop analysis would be the next step. This can be accomplished by coding the TPS_DT in a controller readable programming language and incorporating it in a traffic signal controller as an extended module. Although simulation studies have shown that the proposed optimization methodology with TPS_DT can improve safety and efficiency of the corridor, field studies are necessary to test the methodology before it is considered for field implementation.

References

1. Manual on Uniform Traffic Control Devices: 2009 Edition. FHWA, U.S. Department of Transportation, 2009.

2. Guoyuan Wu, Irene Li, Wei-Bin Zhang, Scott Johnston, Meng Li, Kun Zhou. SPRINTER Tail: Grade Crossing/Traffic Signal Optimization Study. California PATH Research Report UCB-ITS PRR-2009-21. Institute of Transportation Studies, University of California, Berkeley, 2009.

3. Jacobson, M., S. Venglar, and J. Webb. Advanced Intersection Controller Response to Railroad Preemption-Stage I Report. Texas Transportation Institute, Texas A&M University, College Station, Texas, May 1999.

4. Engelbrecht R., S. Venglar, and M. Jacobson. Advanced Intersection Controller Response to Railroad Preemption – Stage II Report. Texas Transportation Institute, Texas A&M University, College Station, Texas, September 1999.

5. Venglar, S., R. Engelbrecht, and S. Sunkari. Advanced Intersection Controller Response to Railroad Preemption – Stage III Report. Texas Transportation Institute, Texas A&M UnivKimersity, College Station, Texas, January 2000.

6. Venglar, S. Advanced Intersection Controller Response to Railroad Preemption –Stage IV Report. Texas Transportation Institute, Texas A&M University, College Station, Texas, February 2000.

7. Zhang, Li. Optimizing Traffic Network Signals Around Railroad Crossings. PhD Dissertation. Virginia Polytechnic Institute and State University, May 2000.

8. Cho, H. Preemption Strategy for Intersections near Highway-Railroad Crossings. Ph.D. Dissertation, Texas A&M University, College Station, TX, 2003.

9. Cho, H. and L.R. Rilett. Improved Transitional Preemption Strategy For Signalized Intersection near At-Grade Railway Crossing, Journal of Transportation Engineering Volume 133, Number 8, American Society of Civil Engineering, Reston, VA, August, 2007, pp 443-454.

10. Korve, Hans W. Traffic Signal Operations near Highway-Rail Grade Crossings. National Cooperative Highway Research program Synthesis 271, NCHRP, Transportation Research Board, National Research Council, Washington D.C. 1999.

11. Elizabeth G. Jones, Aemal H. Khattak, Laurence R. Rilett. The University Nebraska-Lincoln's Highway Rail Grade Crossing Test Bed System. In Transportation Research Record: Journal of the Transportation Research Board. CD-ROM.Transportation Research Board of the National Academics, Washington, D.C., 2009.

12. Cho, H. and L.R. Rilett. Analysis of Performance of Transitional Preemption Strategy for Traffic Signal near At-Grade Railway Grade Crossing. In CD-ROM, Transportation Research Board 88th Annual Meeting, Washington, D.C., January 2009.

13. D. Franca. Estimation Train Arrival Times at Highway-Railroad Grade Crossings Using Multiple Sensors. Master Thesis, University of Nebraska, Lincoln, NE, 2009.

14. Institute of Transportation Engineers (ITE). Preemption of Traffic Signals near Railroad Crossings. Washington, D.C. 2006.

15. Steve P. Venglar P.E., Marc S. Jacobson, Srinivasa R. Sunkari, Roelof. J. Engelbrecht, and Thomas Urbanik II P.E. Guide for Traffic Signal Preemption near Railroad Grade Crossing. Project No 0-1439, Texas Transportation Institute. College Station, Texas, September, 2000.

16. United States. Code of Federal Regulations. Subtitle B, Chapter II, Section 49, Part 234.225. Government Printing Office, Washington, D.C., 1998.

17. Engelbrecht, R.J. The Effect of Variation in Railroad Warning Time on Traffic Signal Preemption. Presented at the Sixth International Symposium on Railroad-Highway Grade Crossing Research and Safety, Knoxville, TN, October 2000.

18. J.M. Tydlacka. A Microsimulation Analysis of Highway Intersections Near Highway-Railroad Grade Crossings. Master Thesis, Texas A&M University, College Station, TX, August, 2003.

19. Peter S. Marshall and William D. Berg. Evaluation of Railroad Preemption Capabilities of Traffic Signal Controllers. In Transportation Research Record No. 1254, TRB, National Research Council, Washington, D.C., 1990, pp. 44-49.

20. Jacob R. Yohe and T. Urbanik. Advance Preempt with Gate Down Confirmation: A Solution for the Preempt Trap. In CD-ROM, Transportation Research Board 86th Annual Meeting, Washington, D.C., January 2007.

21. WBAPS 2005 Web Accident Prediction System. Accident Prediction Report for Public at-Grade Highway-Rail Crossings. U.S. Department of Transportation, Federal Railroad Administration, 2006. 64.80.98.236/wbaps/Location.asp. Accessed 10/31/13.

22. VISSIM 5.40-01- COM Interface Manual. PTV Plannung Transport Verkehr AG, Nov, 2011.

23. B. Park. Development of Genetic Algorithm-Based Signal Optimization Program for Oversaturated Intersections. PhD Dissertation. Department of Civil Engineering, Texas A&M University, College Station, TX, 1998.

24. Zaher K. Khatib and Fusan Lin. Calculations and Evaluations of Traffic –Controller Parameters: Force Off and Permissive Periods. ITE Journal, May 2000.

25. B. Park., C.J. Messer and T. Urbanik II. Traffic Signal Optimization Program for Oversaturated Conditions: Genetic Algorithm Approach. In: TRB 1683, Advanced traffic management systems pp. 133-142. 1999, Washington, D.C.

26. Chun Shao, Adaptive Control System for Isolated Intersection and Traffic Network. PhD Dissertation. University of Akron, Akron, May, 2009.